Precipitation and processing of solids from high pH, high Si groundwater

Rupal Pandya

A thesis submitted in partial fulfillment of the

requirements for the degree of

Master of Science in Civil Engineering

University of Washington

2015

Committee:

Mark Benjamin

Gregory Korshin

Mike Dodd

Program Authorized to Offer Degree:

Department of Civil and Environmental Engineering

University of Washington

Abstract

Precipitation and processing of solids from high pH, high Si groundwater

Rupal Pandya

Chair of the Supervisory Committee:

Prof. Mark Benjamin

Department of Civil and Environmental Engineering

This research is concerned with the treatment of highly contaminated groundwater from the former Occidental Chemical Corporation manufacturing site at Tacoma, WA. During various stages of production that took place at this site from 1927 till mid-1980's, highly caustic brines and chlorinated solvents were released into the ground resulting in widespread contamination of groundwater, notably the elevation of its pH to > 12 and the presence of volatile organic compounds (VOCs) across the site. Elevated pH of the groundwater has resulted in the dissolution of significant amounts of Si (concentrations as high as 48000 ppm). This silica could precipitate on granular activated carbon (GAC) used for VOC removal. This necessitates Si removal from high pH, high Si groundwater before VOC treatment, when this groundwater is extracted and treated *ex-situ*. On the other hand, groundwater can also be acidified *in-situ* to precipitate Si containing solids in the aquifer and form a hydraulic barrier to prevent contaminant plume propagation.

In this study, groundwater samples from the site were analyzed for Si and various other elements. Visual Minteq modelling was used to predict and interpret observed concentration vs pH trends for Si, Al, Ca and Mg. Experiments were conducted to study the precipitation of dissolved Si by acidification and $CaCl_2$ addition. A treatment approach was explored that reduced the volume of generated solids (that would require handling and disposal) to 16% of the groundwater volume. The generated solids were analyzed to be 82% SiO_2, indicating that they might find application in the cement industry. Experiments to study the formation and stability of a hydraulic barrier in a laboratory scale set-up indicated that *in-situ* precipitation can be induced, but the effects on hydraulic conductivity of the soil are difficult to predict.

Table of Contents

List of Figures

List of Tables

List of abbreviation

AOC	Administrative Order on Consent
BGS	Below Ground Surface
cis-1,2-DCE	cis-1,2-Dichloroethylene
cVOC	Chlorinated Volatile Organic Compounds
DI	Deionized
DOC	Dissolved Organic Carbon
DOE	Department of Ecology
EPA	Environmental Protection Agency
GAC	Granular Activated Carbon
ICP-MS	Inductively Coupled Plasma Mass Spectrometer
OCC	Occidental Chemical Corporation
NPDES	National Pollutant Discharge Elimination System
P & T	Pump and Treat
PCE	Tetrachloroethylene
PES	Poly Ether Sulfone
PPB	Parts Per Billion
PPM	Parts Per Million
RCRA	Resource Conservation and Recovery Act
TCE	Trichloroethylene
TGA	Thermogravimetric Analyzer

TIC	Total Inorganic Carbon
TOC	Total Organic Carbon
USEPA	United States Environmental Protection Agency
UW	University of Washington
VM	Visual Minteq

Chapter 1 Project background

The research described herein deals with the groundwater contamination at the former Occidental Chemical Corporation (OCC) property located at 605 Alexander Avenue in Tacoma, WA. Most of the information presented in this chapter is obtained from the Remediation System Evaluation document prepared by Office of Solid Waste and Emergency Responses of the USEPA ("Remediation System Evaluation," 2004). The site occupies 37 acres and is located along the Hylebos waterway. Figure 1.1 shows the site and the surrounding area along with waterways. OCC operated a chlorinated solvent plant on this site between 1947 and 1973. The chemical manufacturing has been discontinued, but OCC has retained the environmental liability.

During various stages of production (processing, transport, storage or disposal), caustic material (e.g. caustic soda and spent or unspent lime from processing activities) and chlorinated solvents (effluents from tetrachloroethylene [PCE] and trichloroethylene [TCE]) were released into the ground. Caustic material, being denser than water, migrated downward to create a high-pH "blob" at depths of 100-160 ft. Contamination of groundwater by high pH and chlorinated volatile organic compounds (cVOCs) is widespread across the site.

Because of the elevated pH, Si and other metals have dissolved into the groundwater, in some cases at high concentrations. In addition to the cVOCs that were released directly (PCE and TCE), the groundwater contains their breakdown products, including cis-1,2-dichloroethylene (cis-1,2-DCE) and vinyl chloride.

The contaminated groundwater migrates and ultimately discharges to the Hylebos and Blair waterway. A milky seep with pH between 8 and 11.2 and containing white solids (presumed to be Ca and Mg precipitates resulting from mixing of high pH groundwater with waterway) has been observed entering the Hylebos waterway. Human exposure to these contaminants is expected through consumption of fish caught in waterway. The contaminated plume is expanding beyond the site, and the shallow groundwater at properties south of the site have been found to be contaminated by PCE and high pH.

Figure 1.1 Site location map ("Remediation System Evaluation," 2004)

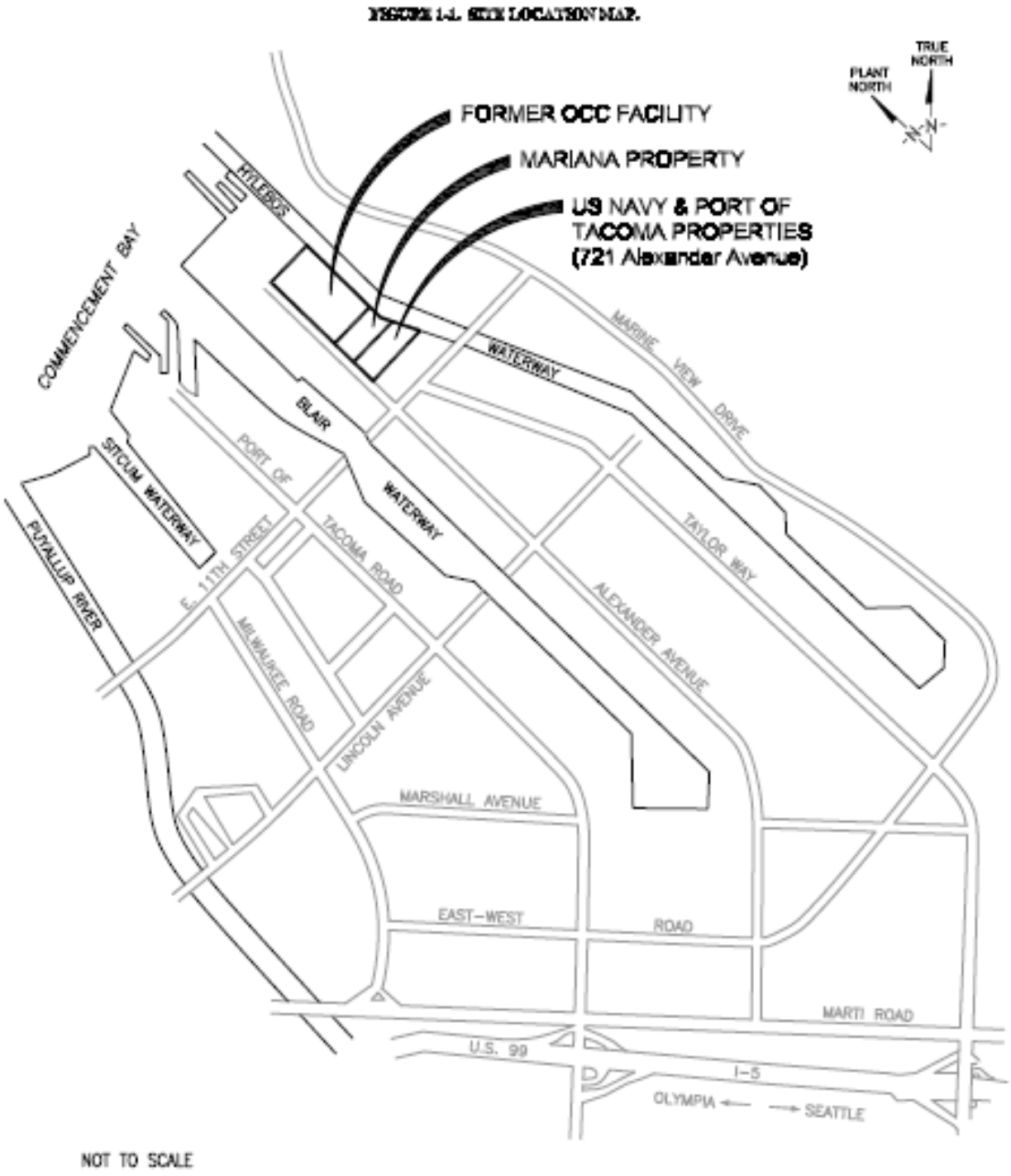

A pump and treat (P&T) system has been in place to extract and treat contaminated groundwater since 1996. A small portion of the treated water is reinjected to the subsurface along the Hylebos waterway to provide a hydraulic barrier against discharges and the remaining treated water is discharged to the Hylebos waterway under a NPDES permit. Although the P&T system is designed to treat high pH groundwater by pH adjustment and accompanying solids removal, current system treats only contaminated groundwater at near neutral pH. Extraction of high pH (>9.5 s.u) groundwater is problematic because of rapid fouling of the wells due to *in-situ* solid precipitation. Also, high pH groundwater could interfere with operation of granular activated carbon (GAC) column used for cVOC removal. It also causes fouling at the injection sites limiting the amount of water that can be injected and interfering with formation of a hydraulic barrier formation between the contaminated site and the waterway.

The Environment Protection Agency's (EPA) Resource Conservation and Recovery Act (RCRA) program provided remediation oversight until 1998; currently Washington State Department of Ecology (WA DOE) is overseeing the development of the site remediation plan. The EPA Superfund program is also working with DOE to develop a remediation plan for the contaminated sediment and to prevent further contamination and discharges of contaminated groundwater into the waterways above regulatory thresholds.

OCC has been working with DOE and EPA to address environmental issues at the site under an Administrative Order on Consent (AOC). The University of Washington (UW) has been engaged to conduct a study to help the key parties develop remediation plan for the site. Key components of the study include:

a) Understanding the effects of high pH on contaminant mobility in the groundwater,

b) Characterizing the precipitation of silica from high pH groundwater and its implications for treatment options, including the formation and stability of an *in-situ* hydraulic barrier,

c) Investigating the potential methods for long term extraction of high pH groundwater

The research described in this thesis deals with potential *ex-situ* treatment options for silica and potential formation of an *in-situ* hydraulic barrier.

Investigation of effects of high pH on groundwater contaminant mobility has already been completed as a separate study and investigation of long term successful extraction of high pH groundwater (through column experiments) is being studied in parallel to this research.

The elevated pH of the groundwater is likely to have dissolved heavy metals and other elements from the aquifer materials into the groundwater in addition to silica. Presence of these toxic substances, especially heavy metals and their release into nearby waterways is hazardous to aquatic life. Therefore, complete analysis of the groundwater to determine the presence of these contaminants was completed to gain an adequate understanding of the relevant chemical equilibria and thereby to gain a more detailed understanding of the system. Also, knowledge of the groundwater's composition is equally important to design and carry out experiments with synthetic solutions prepared to mimic the behavior of the real groundwater in column and related laboratory-scale studies. The presence of few important analytes e.g. Si, Al, Mg and Ca in the groundwater were also modeled using Visual Minteq in order to interpret the concentration levels and trend in the groundwater.

During *ex-situ* treatment of this high pH, high Si groundwater, Si precipitation could foul the GAC used for VOC removal and it can also cause other problems in the treatment train. In addition, pH reduction will be required before discharge of the water into nearby waterways or reinjection into the ground. Thus, removal of Si from the groundwater might be essential before VOC treatment. Accordingly, experiments were carried out to study precipitation of Si by incremental acidification or salt addition ($CaCl_2$). The percent Si precipitation and the volume and morphology of the solids generated were investigated.

Since *ex-situ* treatment is likely to generate a very large amount of solids, experiments were conducted to investigate an approach for substantially reducing the mass and volume of precipitated solids that would have to be handled, processed and disposed of.

On the contrary, *in-situ* precipitation of Si might be useful for forming a hydraulic barrier that could be useful to prevent the propagation of the contaminant plume. Stability of these solids against contact with high pH, low Si groundwater was studied. Experiments exploring the possible formation of the hydraulic barrier in the laboratory scale soil column by injection of varied concentration of neutralizing solution and its stability are underway.

Chapter 2 Materials and methods

2.1 Provenance of groundwater samples and soil cores

The groundwater and soil core samples used in the experiments were obtained from the OCC site during borehole drilling in July, 2014. Three boreholes were drilled in the vicinity of monitoring Well 46-C, Well 82 and Well 83-C, and the soil core samples were collected at depths of up to 150-ft. Groundwater samples were collected from monitoring Wells 46-C, 82, and 83-C and extraction Well #7 at depths up to 130-ft. Soil cores and groundwater from Wells 82, 83-C and Well #7 are expected to be strongly affected by high pH, high Si groundwater as they are close to the source area and in the direction of the plume propagation. Being farther from the source area, soil cores and groundwater from Well 46-C are expected to be less affected.

2.2 Chemicals and consumables

Chemicals

Ultra-pure deionized (DI) water (18.2 MΩ-cm) produced by a Milli-Q system (EMD Millipore, Billerica, MA) was used for solution preparation, dilutions, rinsing and related purposes. Hydrochloric acid (12 mol/L, Macron Fine Chemicals™, Avantor Performance Materials, Center Valley, PA) was diluted to 2 mol/L and was used to acidify the groundwater and to study solids' precipitation. Calcium Chloride powder (Acros Organics, NJ) was used as a salt to precipitate solids from groundwater by salt addition. NaOH pellets (Fisher Scientific, Fairlawn, NJ) were used to prepare 5 mol/L NaOH solution to study the dissolution of solids. Sodium Bicarbonate powder (J.T. Baker, Phillipsburg, NJ) was used to prepare varied concentrations of neutralizing solution to induce precipitation for hydraulic barrier formation. Sodium Chloride crystals (EMD Chemicals, Gibbstown, NJ) were used to prepare the benign solution to establish baseline pressure drop and study stability during hydraulic barrier formation experiments. Calibration standards for all analytes (listed in Table 2.2.1) were prepared using ICP-MS grade analytical standards (Ultra Scientific, Kingstown, RI). Trace metal grade HNO_3 (Fisher Scientific, Fairlawn, NJ) was used to acidify all samples and calibration standards to 1% HNO_3 for ICP-MS analyses. EPA method 6020a internal standard solution (Ultra Scientific, Kingstown, RI) was used as a source of Ge- as an internal standard.

Table 2.2.1 Analytes quantified in Oxy site groundwater

Analytes (ion mass)	Analytes (ion mass)
Aluminum (27)	Barium (138)
Arsenic (75)	Calcium (42,44,48)
Cadmium (114)	Magnesium (24)
Chromium (52)	Manganese (55)
Copper (63)	Silicon (28)
Iron (54,56,57)	Strontium (88)
Lead (208)	Vanadium (51)
Nickel (58)	Zinc (64,66,68)
Thallium (205)	

Glassware and Consumables

Glassware was cleaned by soaking in 20% reagent-grade HNO_3.

Polypropylene centrifuge tubes (15-ml and 50-ml) were used to collect samples from experiments, to prepare calibration standards and samples for ICP-MS analyses. Samples were withdrawn from the centrifuge tubes with a 10-ml Luer-Lok tip disposable syringe (Becton, Dickinson & Company, Franklin Lakes, NJ) connected to a stainless steel needle. Poly Ether Sulfone (PES) filters with nominal 0.45-μm pores (VWR International, Radnor, PA and Whatman, GE Healthcare and Lifesciences, Piscataway, NJ) were used to filter all samples to avoid clogging of the ICP-MS nebulizer. Serological pipettes, and tips for various micropipettes were also used to draw and transfer samples as needed.

2.3 Analytical Instruments

A PerkinElmer Elan DRC-e Inductively Coupled Plasma Mass Spectrometer (ICP-MS) was used to analyze the constituents listed in Table 2.2.1.

A thermogravimetric analyzer (TA Instruments, model TGA Q50, with EGA furnace) was used to characterize the amount and strength of water binding to the solids generated by acidification of Oxy site groundwater. Advantage Software (Universal Analysis 2000, v4.5A) was used to analyze the data.

A high-pH, double-junction pH electrode (Model: 5994-23, Cole-Parmer, IL) was used in combination with an advanced electrochemistry meter (Orion™ Versa Star, Thermo Scientific) to measure pH of the suspension/solution during experiments. The pH electrode was calibrated with buffer solutions (pH 4, 7 10 from Thermo Fisher Scientific, Chelmsford, MA and pH 12.45 from Ricca Chemical Company, Arlington, TX).

The pressure drop across the soil column was recorded with a data acquisition/data logger system (Model: 34970A, Agilent Technologies, Santa Clara, CA).

2.4 Analytical Methods

2.4.1 ICP-MS Analyses

2.4.1.1 Challenges with ICP-MS analyses

A high concentration of matrix elements can either suppress or enhance the signals of other trace-level analytes (Tan and Horlick, 1987). Since the Oxy site groundwater has a very high concentration of Si, ICP-MS analyses for trace-level analytes in this matrix could be affected. In addition, significant instrumental drift was observed for the analytes during the initial analytical runs that utilized an external calibration method (calibration standards prepared in DI water). This could have been caused by the presence of high concentrations of solutes resulting in instrument sensitivity changes between the calibration standards and samples ("ELAN Software Reference Guide," 2008).

To minimize the aforementioned problems, many of the samples were diluted prior to analysis. An acceptable range of dilution factors for most of these samples was determined by experiments that quantified spike recovery of each analyte listed in Table 2.2.1 (5 ppm to 30 ppm for Si, 2 ppb to 200 ppb for other analytes) in Well # 7 groundwater at varying dilutions. The high Si concentration in Well # 7 groundwater required dilution of the groundwater by a factor of at least 800. Also, to eliminate the sensitivity drift caused by matrix differences between the calibration standards and the samples, a standard addition calibration method (standards prepared by spiking one of the diluted sample with known concentrations of each analyte) was used in the analyses ("ELAN Software Reference Guide," 2008). Figure 2.4.1.1.1 summarizes the analytical procedure when standard addition calibration was used.

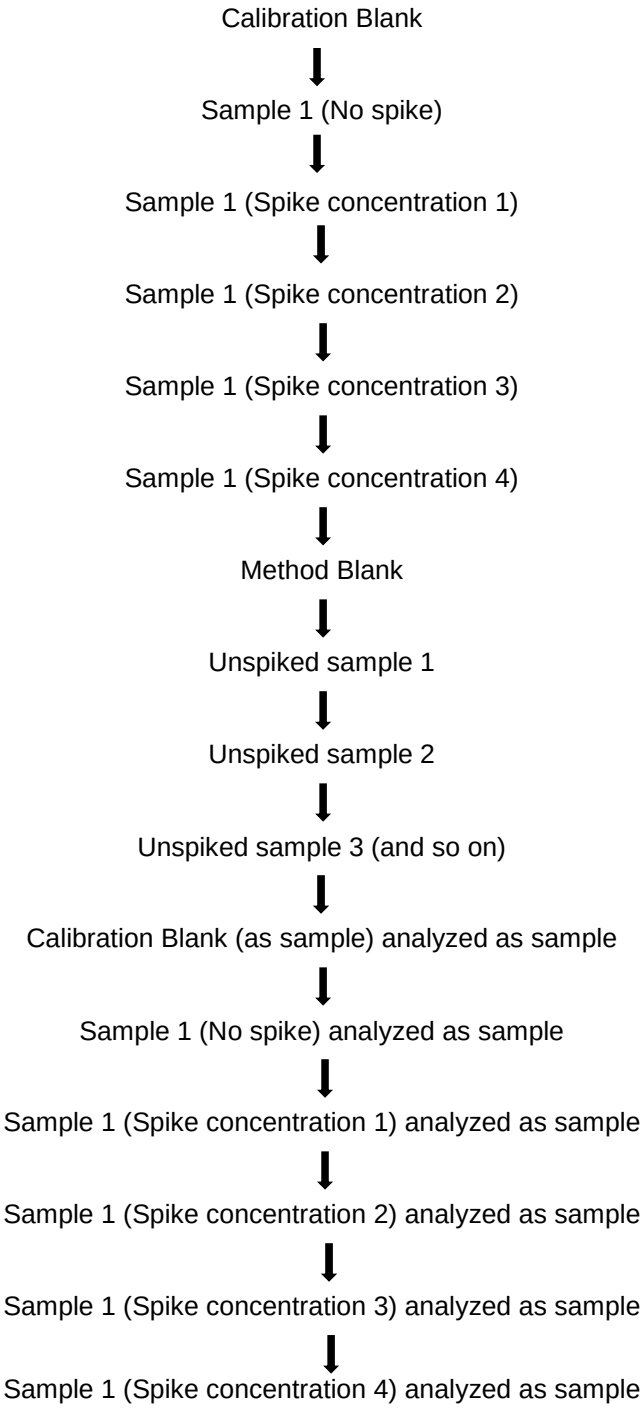

Figure 2.4.1.1.1 Measurement procedure when using standard addition calibration

In addition, an internal standard was used to correct for instrument sensitivity changes from sample to sample. Examination of the results from initial analytical runs revealed a significant background level of recommended internal standards ("Inductively Coupled Plasma Mass Spectrometry, EPA Method 6020a," 2007) other than Ge in the groundwater. Therefore, Ge (ion mass 74) was chosen as an internal standard for each analyte studied. As recommended in EPA method 6020a, a method blank was also analyzed to monitor possible contamination resulting from the reagents, other articles (e.g. filters) and equipment (employed for sample preparation).

2.4.1.2 Sample preparation for ICP-MS analyses

The following steps were followed to prepare samples, calibration standards and blanks for ICP-MS analyses.

1. All glassware was rinsed with DI water, soaked in 20% HNO_3 for at least 8 hour, rinsed three times with DI water and allowed to dry before use.

2. New centrifuge tubes, syringes, filters and needles were used to prepare samples and calibration standards.

3. One of the samples was diluted 8000x with DI water except during groundwater analyses, when one of the samples was diluted 800x. Trace metal grade HNO_3 was added to this dilution so that it was 1% HNO_3 (by vol). The dilution was filtered through 0.45-μm PES filter. The first 3 ml of filtrate was discarded and the rest was collected.

4. Calibration standards (10 ppm to 50 ppm Si/Ca and 10 ppb to 100 ppb for other analytes) were prepared by diluting ICP-MS grade analytical standards of each analyte with the diluent prepared in step 3.

5. The groundwater samples collected in the field and the samples from experiments were diluted 800x with DI water and acidified and filtered as described in step 3.

6. Two 1% HNO_3 solutions were prepared. One of these solutions was used as a calibration blank, and the other was filtered through a 0.45 μm PES filter and used as a method blank.

7. Ten ml of each diluted sample, calibration standard, method blank and calibration blank was transferred to a centrifuge tube using a new serological pipette. The solutions were spiked with 50 μl of 2 ppm EPA method 6020a internal standard solution.

8. The solutions described above were analyzed using ICP-MS.

2.4.1.3 Calibration and calculation steps

The following steps were followed to prepare calibration curves, calculate instrument drift, estimate analyte recovery, and ultimately to determine the concentration of each analyte in experimental and field samples.

1. The net ICP-MS signal intensity for each analyte in each sample was calculated based on the difference between the relative intensity (measured intensity for the analyte divided by measured intensity for internal standard) of that particular analyte in the sample and the calibration blank. Table 2.4.1.3.1 shows an example of this calculations.

2. A calibration curve for each analyte was prepared by plotting the net intensity vs. the known spike concentration of that analyte in the calibration standards. The slope of the calibration curve represents the instrument sensitivity for a unit change in analyte concentration.

3. The slope thus obtained was used to calculate the concentration of the analyte in samples with unknown concentrations (by dividing the calculated net intensity of the analyte in the unknown sample by the slope of calibration curve for that analyte).

4. The calibration standards were reanalyzed at the end of each ICP-MS run (Figure 2.4.1.1.1) to estimate the instrument sensitivity drift and the percent recovery for all analytes. Instrument sensitivity drift was estimated as the fractional change in slope of the curve (net intensity vs concentration) between the initial and final analyses. The fractional recovery was estimated as the fraction of the known spike concentration that was recovered when the calibration standards were reanalyzed.

Table 2.4.1.3.1 Example calculation to find the net intensity

	Analyte Si	Ge (Internal standard)	Net Intensity of Si in sample / standard solution
Calibration blank			
Measured intensity	86506	94253	
Sample/standard solution			
Measured intensity	218227307	97503	(218227307 / 97503) – (86506 / 94253) = 2237.2

5. The analytes present in the method blank were subtracted from the respective analyte concentrations in samples to account for leaching of that analyte from the filter.

2.4.2 TGA Analyses

Thermogravimetric analyses of solids generated by the acidification of Oxy site groundwater were conducted to determine the temperature at which the solids lost water of hydration and thereby determine the temperature for processing the solids prior to their transport and disposal. The solids generated by acidification were stored in a water-tight container and analyzed, whenever possible, on the day of their preparation. The steps in this analysis were as follows.

1. A flake of solid was placed in the platinum crucible for analysis.

2. Dry air at a flow rate of 90 mL/min across the sample was used as the purge gas.

3. The temperature of the sample compartment was increased at a rate of 5^{o}C/min, starting at room temperature, and continuing until the temperature was 110^{o}C. The sample was held at each incremental temperature for 5 min before raising the temperature to the next level, except for a specified isothermal period at selected temperature.

4. The instrument reported the weight of the solid as a function of temperature.

2.5 Experiment methods

2.5.1 Si Precipitation from Oxy site groundwater

Si can be precipitated out of high pH, high Si groundwater if its pH is reduced. Si precipitation can also be initiated and enhanced by addition of nucleation sites e.g. cations (Gorrepati et al., 2010).

Preliminary experiments had suggested that volume and morphology of the solids generated depend on the reaction conditions, such as temperature, mixing speed, and acid/salt addition rates. All the experiments described here were conducted at room temperature and mixing speed was maintained to ensure vortex formation and hence efficient mixing. Both, acid and salt addition experiment were carried out at slow and rapid addition rates. The following sections describe the procedure used in the acidification and salt addition experiments.

Groundwater from Well 82 at a depth of 100-ft and Well 7 at a depth of 130-ft were selected for this experiment, because those samples had highest pH (Well 82-100: pH 11.64 and Well 7: pH 11.6, Table 3.1.2.1). Both samples appeared to be highly contaminated (the water was black), as shown in Figure 2.5.1.1.

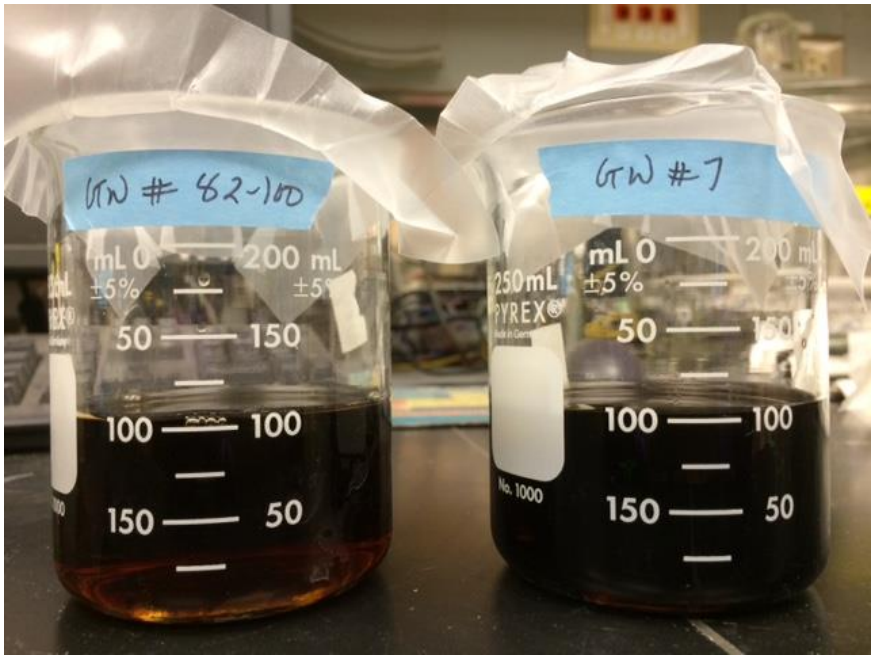

Figure 2.5.1.1 Visual Appearance of groundwater from Well 82 at depth 100-ft and Well 7 at depth 130-ft

2.5.1.1 Acid Addition

The slow acid addition to groundwater from Well 82 at depth 100-ft followed steps below.

1. The pH probe was calibrated before its use in the experiment.
2. Groundwater (100-ml) was acidified using 2 mol/L HCl. Both the groundwater and the acid were at room temperature (T=18 – 20^{o}C).
3. The mixture was continuously stirred during acid addition except during pH measurement and sample withdrawal. Mixing speed was maintained between 220-280 rpm throughout the experiment to ensure formation of a moderately developed vortex; excessively vigorous mixing was avoided. The mixing speed was set at a higher rpm when the suspension thickened because of the presence of solids.
4. Acid was added in small increments (1 to 4-ml in each increment) followed by 15 min of mixing and pH measurement.
5. A sample was withdrawn after each acid addition. The stirring was stopped and suspended solids were allowed to settle before withdrawal of supernatant samples.
6. Withdrawn samples were analyzed using ICP-MS to determine the concentration of dissolved Si in the supernatant. The analyses were done as described in sections 2.4.1.2 and 2.4.1.3.

This experiment was followed by rapid acid addition (12-ml of 2 mol/L HCl solution was added at once to 50-ml of above mentioned groundwater, quantity of acid required during slow acid addition to reduce the pH < 10) to study the volume and morphology of the solids generated.

Visual observations and results of percent Si precipitation at varied pH are presented and discussed in section 3.2.1.

2.5.1.2 $CaCl_2$ addition

The slow $CaCl_2$ salt addition to the Well 7 groundwater at depth 130 ft followed steps below.

1. One hundred ml of groundwater was dosed with about 0.1 g of dry $CaCl_2$ salt in each increment followed by 10-15 min of mixing.

2. The suspension was mixed at higher rpm (260 – 300) than in the acid addition experiment to break the lumps of solids. Mixing was stopped at the time of sample withdrawal.
3. A sample was withdrawn after each $CaCl_2$ addition. The suspension was allowed to settle before sample withdrawal to minimize loss of solids.
4. Samples were analyzed for dissolved Si using ICP-MS by following the steps described in section 2.4.1.2 and 2.4.1.3.
5. The pH of the suspension was measured at the end of the experiment.

This experiment was followed by rapid $CaCl_2$ addition (5g of powdered $CaCl_2$ salt was added at once to 100-ml of above mentioned groundwater).

Visual observations and results of percent Si precipitation with increasing $CaCl_2$ addition are presented and discussed in section 3.2.2.

2.5.2 Treatment and processing of solids generated during *ex-situ* groundwater treatment

The solids precipitated by slow acid addition (as described in section 2.5.1.1) appeared to have incorporated a substantial amount of water. Experiments were conducted to release that water by mechanical squeezing. The dewatered solids thus obtained were examined using thermogravimetric analyses to determine the loss of water of hydration as a function of temperature. A temperature that seemed attractive for drying was then chosen, and the composition of the dried solids was examined. In these experiments, groundwater from Well 82 at depth 100-ft (pH 11.64, Si: 22500 ppm) and from Well 7 at depth 130-ft (pH 11.6, Si: 48000 ppm) was acidified to generate the solids.

2.5.2.1 Precipitation of solids during *ex-situ* treatment

The conditions used for the precipitation step were as follows.

1. 100-ml of groundwater was placed in a beaker and was mixed with a stir bar at a mixing speed of 220-260 rpm.
2. One ml of 2 mol/L HCl was added at 5-min intervals until the pH was reduced to < 10. As shown in Figure 3.2.1.2.1, > 99% of the Si precipitates under these conditions.

3. A supernatant sample was collected at the end of the acidification process and analyzed for dissolved Si.

4. The generated solids were allowed to settle overnight or longer before decanting the supernatant to collect wet solids.

5. The reactor contents were weighed after acid addition and after decanting the supernatant to estimate the weight and yield of wet solids.

Results obtained from these experiments are presented in section 3.3.1.

2.5.2.2 Mechanical squeezing (dewatering) of wet solids and thermogravimetric analyses

Wet solids precipitated and collected as described in section 2.5.2.1 were dewatered by squeezing them between two rollers of a pasta making home appliance to mimic the performance of a larger scale filter press. Figure 2.5.2.2.1 shows this apparatus.

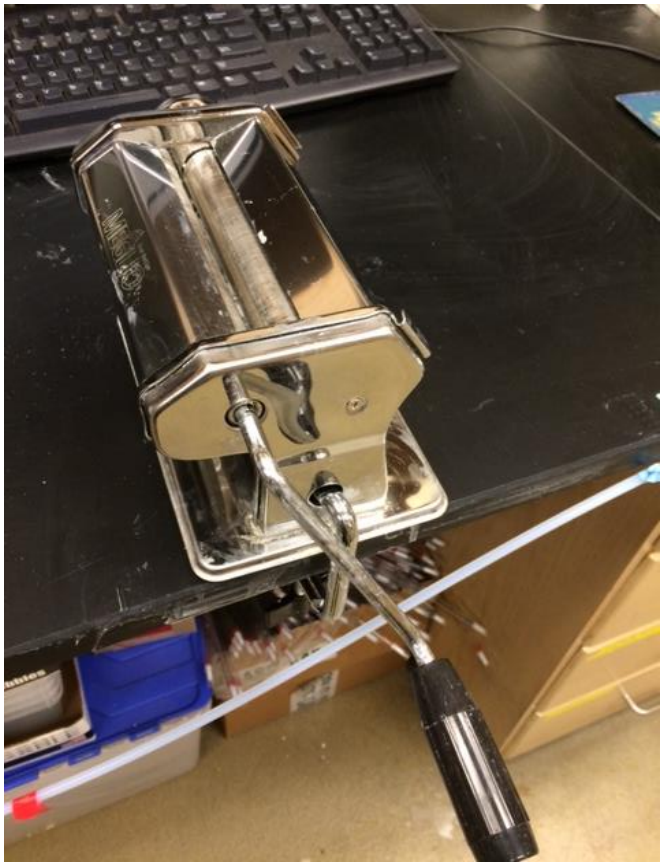

Figure 2.5.2.2.1 Apparatus (Meglio pasta maker) used to dewater precipitated solids from the Oxy site groundwater

The following steps describe the procedure.

1. The cotton fabric was weighed before receiving the wet solids.
2. Wet solids were placed between two layers of fabric and were tamped to generate an approximately uniform thickness.
3. The fabric was weighed after receiving the wet solids.
4. The spacing between two rollers of the apparatus was adjusted such as to squeeze the wrapped solids tightly between the rollers to ensure as much removal of water as possible.
5. The wrapped wet solids were squeezed by passing the fabric containing them through the rollers of the apparatus.
6. The dewatered solids were scrapped off the fabric and weighed.
7. A small sample of dewatered solids was collected in a water-tight container for thermogravimetric analysis.
8. A small weighed sample of dewatered solids was dissolved in a known volume of 5 mol/L NaOH, and the solution was analyzed for dissolved Si using ICP-MS as per the procedure described in section 2.4.1.2 and 2.4.1.3.

The results from this step of the experiment are presented in section 3.3.2.

After choosing a drying temperature based on the TGA results, a new batch of solids was precipitated using groundwater from Well 82 at depth 100-ft and dewatered using the same procedure. These solids were processed as follows to determine the yield and composition of dried solids.

1. The dewatered solids were dried at the selected temperature for about 24 hour and were then weighed.
2. The composition of the dried solids was analyzed as described in step 8 of section 2.5.2.2.
3. Some of the dried solids were crushed to a fine powder.

4. The 2-ml vial was weighed and filled with the powdered solids. The vial was filled as compact as possible, but no external pressure was applied.

5. The vial was weighed, and the apparent density of the dried solids was computed.

The results from this step of the experiment are presented in section 3.3.1 to 3.3.3.

2.5.3 Stability of solids

Stability of the solids generated in the aquifer during possible *in-situ* Si precipitation was investigated by studying the solubility of these solids in 5 mol/L NaOH solution after three different ageing periods.

Three batches of solids were generated by slow acidification of groundwater from Well 82 at depth 100-ft (as per the procedure described in section 2.5.1.1) to pH less than 10. One batch of solids was dissolved in the NaOH solution after 1 hour of precipitation (called freshly precipitated solids). The second batch of solids was allowed to age for about 10 days before dissolution and the third batch of solids was aged for 5.5 months before initiation of dissolution. The pH was periodically monitored during the ageing period. The pH was maintained at less than 10 by addition of 2 mol/L HCl or 5 mol/L NaOH, as required. At the end of the ageing period, the dissolution of solids was carried out by addition of 5 mol/L NaOH solution in small increments, as per the steps described below.

1. The suspension was continuously mixed at 220-280 rpm throughout the dissolution experiment to ensure formation of a moderately developed vortex and to avoid vigorous mixing. Mixing was stopped at the time of pH measurement and sample withdrawal.

2. To study the dissolved Si concentration at few increments in pH between complete Si precipitation and complete dissolution, the suspension was dosed with 5 mol/L NaOH solution in small increments.

3. When the pH was raised by about 0.2 – 0.4 units from the previous pH, a supernatant sample was withdrawn at the end of 1 hour mixing period for Si analysis by ICP-MS (following steps 2.4.1.2 and 2.4.1.3)

The results from this experiment are presented in section 3.4.

2.5.4 Hydraulic barrier formation and its stability experiment

Figure 2.5.4.1 shows the porous ceramic tube used to hold the soil.

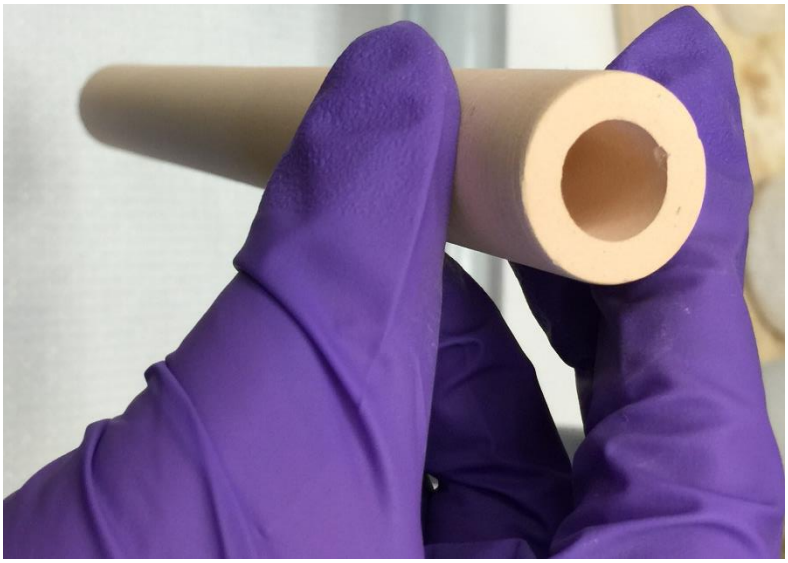

Figure 2.5.4.1 Porous ceramic tube to be filled with soil

The ceramic tube was filled with the soil extracted from the site and was installed in the plexiglass shell (shown in figure 2.5.4.2).

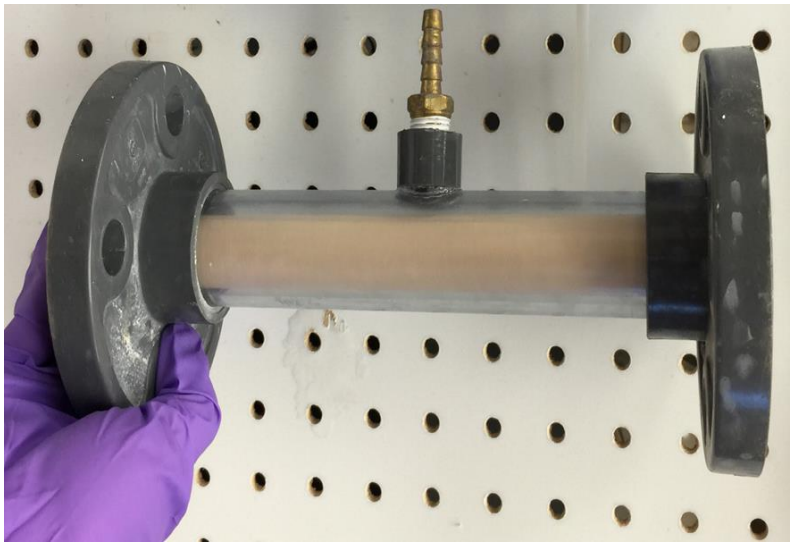

Figure 2.5.4.2 Experiment setup to study hydraulic barrier formation and its stability

The shell side received the neutralizing solution and the tube side received the groundwater flow. The apparatus was sealed on the shell side so that the groundwater that is supposed to flow through the soil does not enter the shell side. There was only one outlet at the downstream end of the apparatus. Neutralizing solution permeated through the ceramic tube into the groundwater passing through the soil. The goal was to uniformly distribute the neutralizing solution through the length of the soil column and generate the Si based solids to form a hydraulic barrier. The pressure transducer in the upstream of the groundwater inlet recorded the hydraulic resistance to flow.

Groundwater from Well 7 extracted at a depth of 130-ft (Si: 48109 ppm) and relatively unaffected soil taken from Well 46C at a depth of 49-ft was chosen to study hydraulic barrier formation. $NaHCO_3$ was used as a neutralizing solution because it is a weak acid, is likely to have less extreme impact at the site of injection and expected to be distributed over a larger area. Batch experiments were conducted to find the threshold volumetric proportion of 1 mol/L $NaHCO_3$ to the Well 7 groundwater for precipitation of solids. These volumetric proportion was used to determine the relative flow rates of $NaHCO_3$ solution to the groundwater.

The following steps describe the experiment procedure.

1. The baseline pressure drop was established by passing the benign solution (4.3 mol/L NaCl, pH 11.6: pH and density similar to Well 7 groundwater) through the soil. The shell side received the $NaHCO_3$ solution during this time.
2. Benign solution was switched to groundwater from Well 7. Benign solution/Groundwater and $NaHCO_3$ solution flow rates were maintained to reach a Darcy velocity of 2.4 cm/min at the end of tube and their relative flow rates were maintained based on the results of batch experiments described earlier. The inlet groundwater pressure was recorded with time.
3. The groundwater and neutralizing solution flows were switched to benign solution (wherever applicable) when the inlet pressure reached about 17 psi to study hydraulic barrier stability.
4. At the end of the experiment, the ceramic tubes were broken to observe the solids precipitation.

The results from this experiment are presented in section 3.5.

Chapter 3 Experiment results and discussion

3.1 Groundwater Analyses

3.1.1 Results

3.1.1.1 Measured pH of the groundwater

Table 3.1.1.1.1 lists the pH values in groundwater samples from different depths in various wells.

Table 3.1.1.1.1 Measured pH of the groundwater extracted from Oxy site

Groundwater from Well # - depth (in ft bgs)	pH s.u.	Groundwater from Well # - depth (in ft bgs)	pH s.u.
7-130	11.60	82-100	11.64
46C-25	9.34	83C-25	6.98
46C-50	8.17	83C-50	6.96
46C-75	7.85	83C-75	7.81
46C-100	8.10	83C-100	9.80
46C-130	7.55	83C-130	11.41
82-30	11.30		

3.1.1.2 Determination of analytes in groundwater

Figure 3.1.1.2.1 thru 3.1.1.2.3 show the calibration curves, net intensity in calibration standards when they were analyzed as a sample with unknown concentration at the end of ICP-MS run, and spike recovery graphs for selected elements. Appendix 1 shows these graphs for rest of the analytes. Table 3.1.2.1 summarizes the percent spike recovery and percent instrument drift for each analyte when the groundwater were analyzed at 800x dilution.

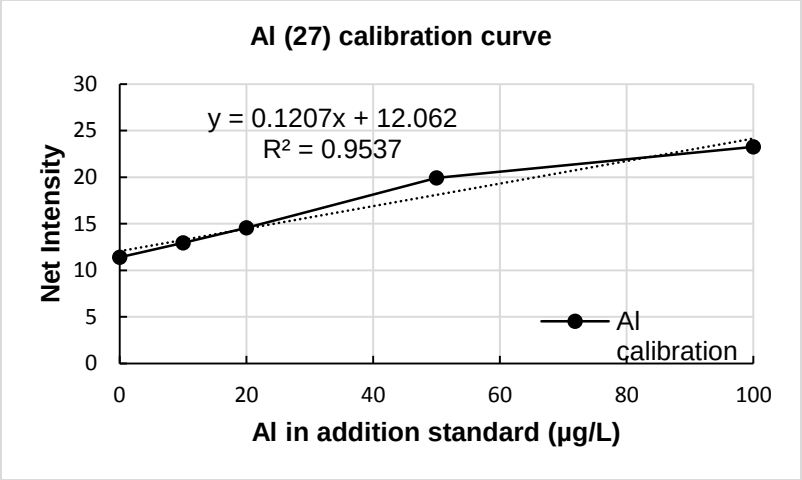

Instrument Sensitivity drift for Al

= % change in slope of net intensity vs concentration in addition standards

= (0.1308 - 0.1207) / 0.1207

= 8.37%

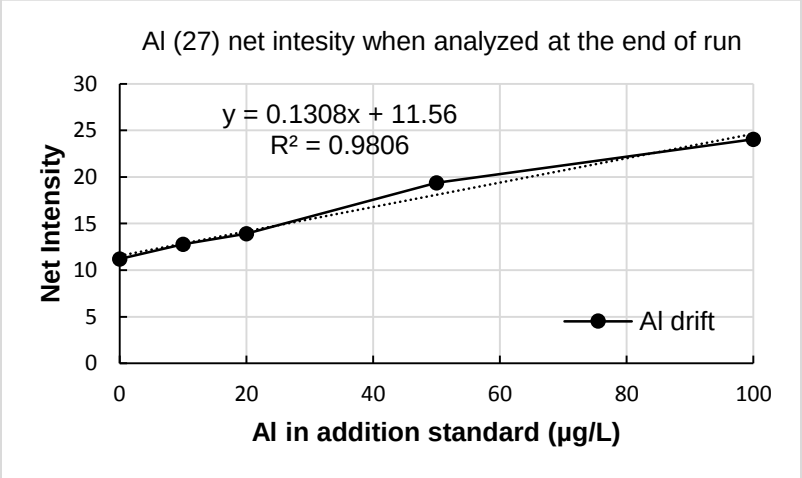

Al recovery

= slope of recovery curve

= 108.4 %

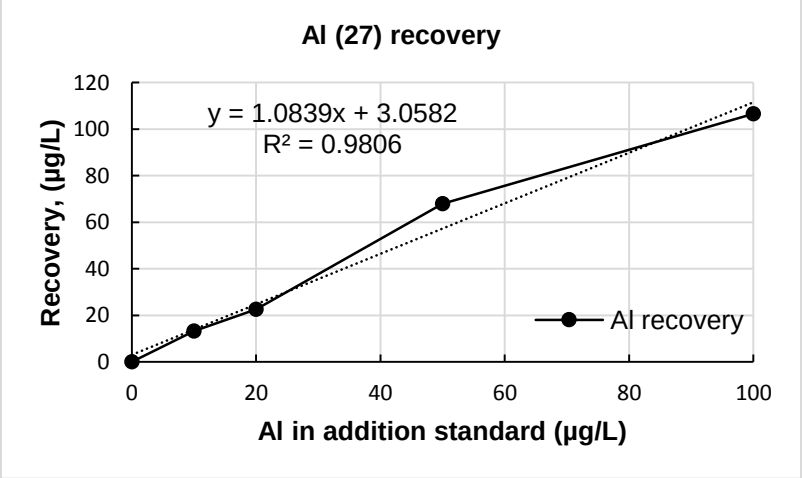

Figure 3.1.1.2.1: Al (27) ICP-MS analytical data: calibration curve, drift and recovery estimation

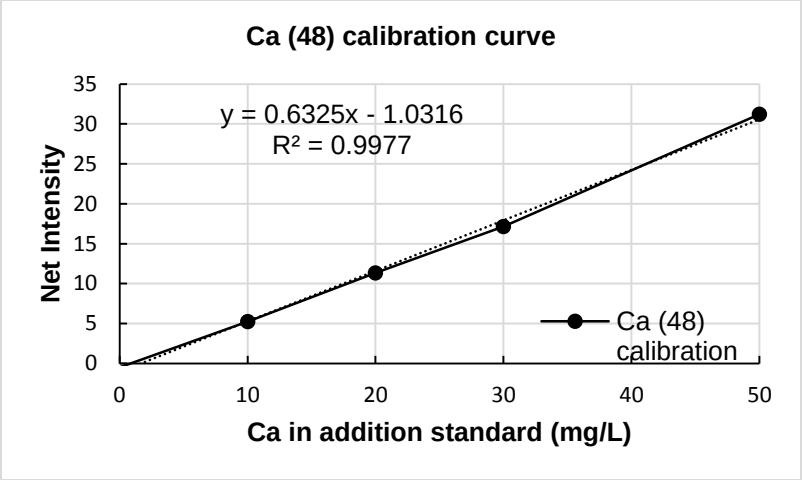

Instrument sensitivity drift for Ca-48

= (0.6311-0.6325)/0.6325

= -0.22%

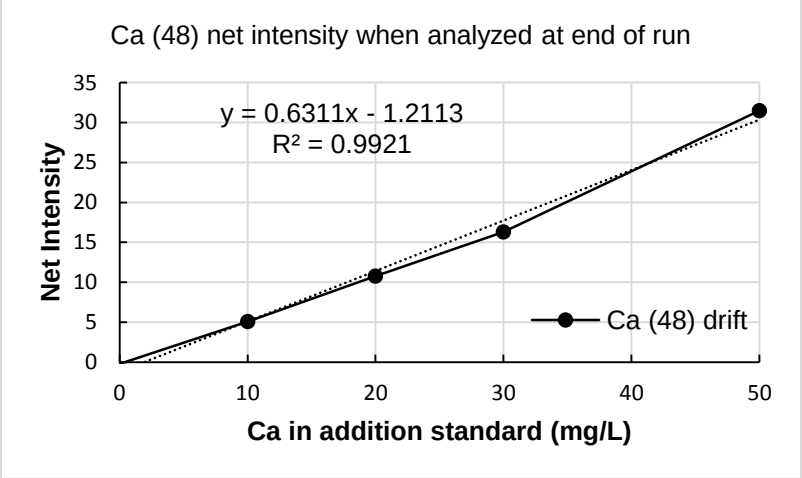

Ca (48) recovery

=99.8%

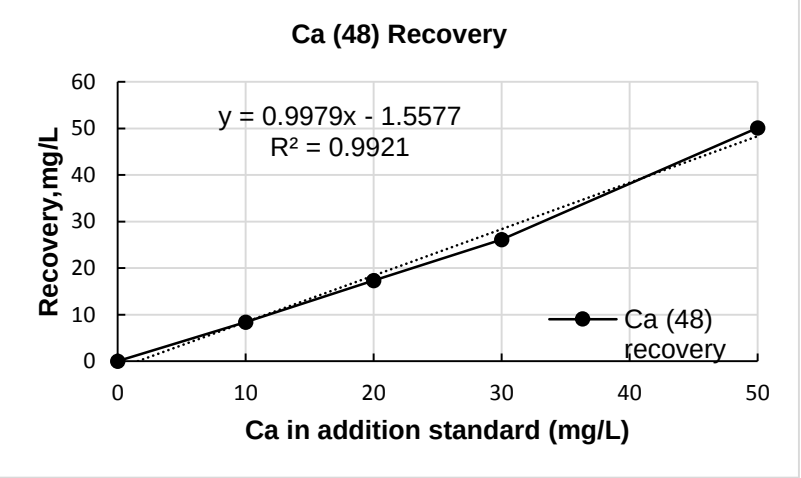

Figure 3.1.1.2.2: Ca (48) ICP-MS analytical data: calibration curve, drift and recovery estimation

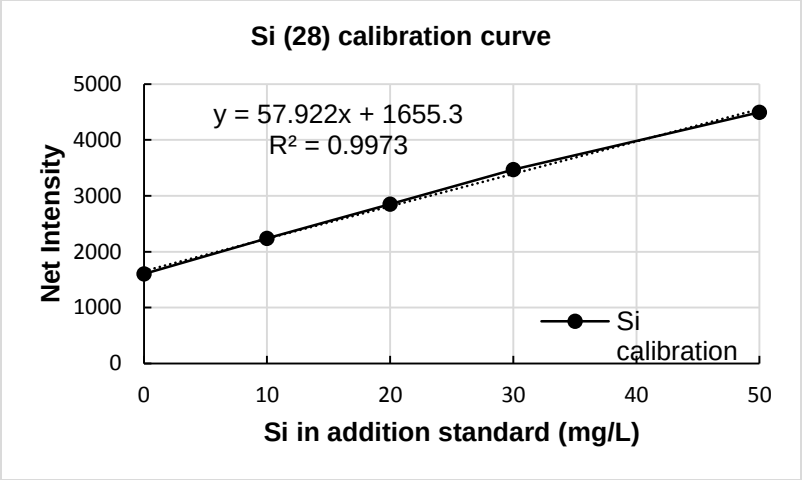

Instrument sensitivity drift for Si

= (60.98 – 57.922) / 57.922

= 5.28 %

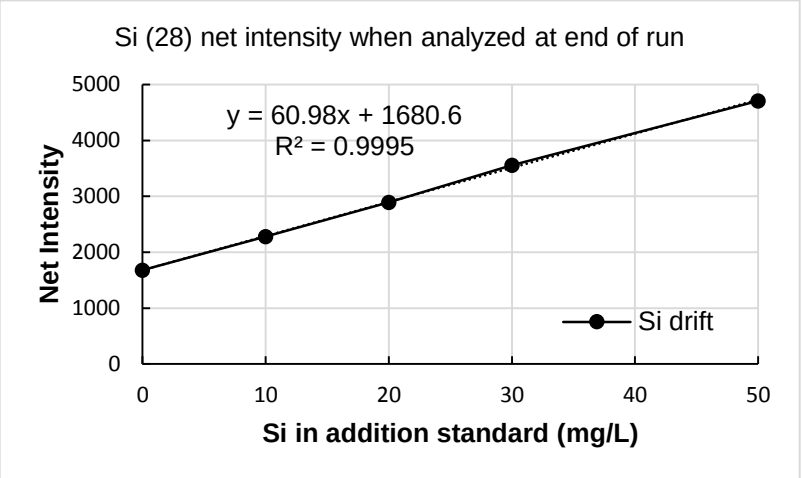

Si recovery

= 105.2 %

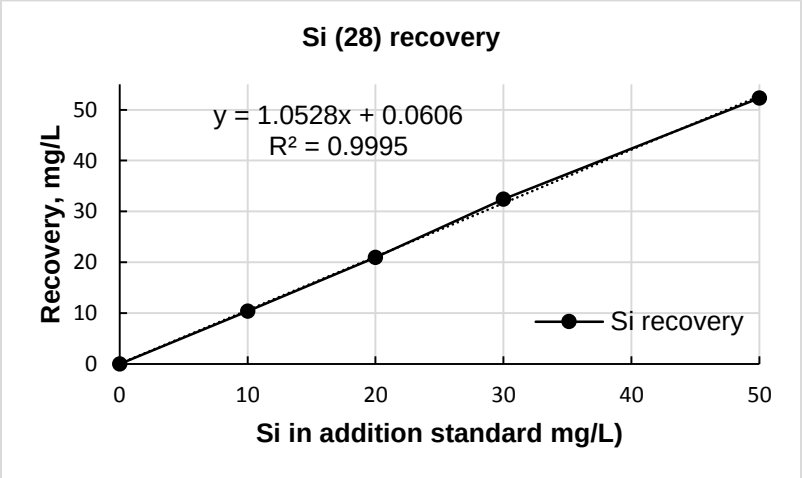

Figure 3.1.1.2.3: Si (28) ICP-MS analytical data: calibration curve, drift and recovery estimation

3.1.2 Discussion

Table 3.1.2.1 also presents concentrations determined for each analyte in the groundwater samples. Groundwater #7 was analyzed separately. Since the groundwater from Well #7 has a significantly higher concentration of Si than the rest of the groundwater samples, addition calibration standards were prepared in 8000x dilution to avoid over saturation of the ICP-MS detector with Si ions. The last two columns of Table 3.1.2.1 present percent spike recovery and percent instrument drift during Groundwater #7 analyses. The percent spike recovery ranged from 96% - 122% and percent drift ranged from -3.7 % to 22%.

The concentration of each analyte follows a consistent trend (increasing or decreasing) with pH. Visual Minteq (http://vminteq.lwr.kth.se/) modeling was used to predict the equilibrium concentration of the analytes and interpret the observed trends for Si, Al, Ca, and Mg.

An input file representing water containing the concentrations of all analyed species at their maximum concentrations in the groundwater (selected from the data for all the groundwater samples, Table 3.1.2.1) was created in Visual Minteq (VM). The model input included the average concentration of total inorganic carbon (TIC), F^-, Cl^-, Br^-, NO_3^-, SO_4^{-2}, and PO_4^{-3}. These anions were analyzed separately (using equipment located in the School of Forestry of the University of Washington) and results of these analysis are presented in Table 3.1.2.2. As evident from the data in Table 3.1.2.2, some of the Oxy site groundwaters (82-100 and 83C-130) contain a significant amount of Total Organic Carbon (TOC). TOC concentrations show an increasing trend with increasing pH. However, because the characteristics of the DOC molecules were not known, the DOC was excluded from VM data input.

Table 3.1.2.1 Groundwater analyses along with percent spike recovery and percent instrument drift

Analyte	UOM	Recovery	Drift	82-100	82-30	46C-25	46C-50	46C-75	46C-100	46C-130	83C-25	83C-50	83C-75	83C-100	83C-130	GW #7	Recovery	drift
																	GW # 7 analysis	
pH				11.636	11.3	9.342	8.173	7.848	8.101	7.551	6.975	6.964	7.814	9.801	11.407	11.6		
Al	ppb	108.4%	8.4%	77621	7032	172	13	46	BD	BD	BD	BD	BD	BD	344663	539823	120.0%	19.6%
As	ppb	99.4%	-0.5%	94	0	BD	BD	BD	0	BD	BD	0	19	94	206	378	99.4%	-0.7%
Ba	ppb	111.0%	11.0%	510	BD	BD	325	565	243	464	500	613	367	10	BD	42	98.1%	-1.9%
Ca (48)	ppm	99.8%	-0.2%	BD	BD	BD	142	169	125	315	385	526	240	4	BD	BD	104.7%	4.7%
Ca(44)	ppm	98.6%	-1.4%	353	47	BD	139	169	129	325	350	489	214	16	558	405	102.3%	2.3%
Ca (42)	ppm	97.3%	-2.7%	1	BD	BD	131	166	140	342	364	525	252	42	15	BD	103.3%	3.3%
Cd	ppb	106.2%	6.2%	BD	6	BD	BD	BD	BD	BD	BD	BD	BD	BD	BD	BD	97.9%	-2.1%
Cr	ppb	103.3%	3.3%	10	90	53	73	43	60	113	123	123	86	123	146	31	102.4%	2.4%
Cu	ppb	102.4%	2.4%	533	43	18	141	110	368	147	61	196	208	760	355	211	99.6%	-0.4%
Fe (54)	ppb	99.1%	-1.2%	515	1216	561	3836	2620	94	1871	421	BD	1591	140	5333	6130	99.2%	-0.5%
Fe (57)	ppb	103.6%	3.3%	331	1058	331	2446	1851	132	1521	1058	992	1521	397	2711	2977	97.2%	-3.1%
Mg	ppb	96.3%	-3.7%	189	76	132	180173	186225	146005	722143	757762	823968	280391	504	BD	134	104.4%	4.3%
Mn	ppb	101.3%	1.4%	2	12	4	366	314	150	540	44	2377	243	BD	BD	56	103.1%	3.1%
Ni	ppb	102.6%	2.6%	BD	BD	BD	0	5	44	146	BD	131	34	BD	44	245	100.5%	0.5%
Pb	ppb	121.5%	21.5%	57	BD	BD	BD	BD	BD	BD	BD	57	BD	BD	BD	71	95.9%	-4.1%
Si	ppm	105.3%	5.3%	22524	3592	BD	BD	BD	BD	BD	BD	BD	BD	107	35749	48109	114.0%	14.0%
Sr	ppb	103.3%	3.3%	220	76	8	2997	3650	2938	6826	6154	9285	5199	919	205	214	102.4%	2.4%
Tl	ppb	122.0%	22.0%	BD	BD	BD	BD	BD	BD	BD	BD	BD	BD	BD	BD	BD	96.0%	-4.1%
V	ppb	104.0%	4.0%	1861	156	BD	261	96	107	89	78	99	198	482	1634	1057	102.8%	2.8%
Zn (64)	ppb	100.5%	0.5%	BD	BD	BD	BD	BD	BD	BD	BD	BD	BD	BD	BD	1727	106.0%	6.0%
Zn (66)	ppb	99.1%	-0.9%	BD	BD	BD	BD	BD	BD	BD	BD	BD	BD	BD	BD	1765	104.5%	4.5%
Zn (68)	ppb	98.7%	-1.2%	BD	BD	BD	BD	BD	BD	BD	BD	BD	BD	BD	BD	1862	103.2%	3.2%

BD Below detection

Table 3.1.2.2 TOC and important anion concentrations in the Oxy site groundwater extracted (Courtesy: School of Forestry, University of Washington)

Groundwater	pH	TIC	TOC	F	Cl	Br	NO3-N	PO4-P	SO4-S
		ppm	ppm	ppm	ppm	ppm	ppm	ppm	ppm
46C-25	9.34	847.4	6.8	6.3	12.3	ND	16.0	0.7	2.8
46C-50	8.17		29.7	9.5	12411.0	ND	21.6	4.1	0.7
46C-75	7.85	123.6	24.5	64.1	19303.0	ND	49.2	ND	0.8
46C-100	8.10	91.2	20.0	75.3	24396.0	ND	90.4	7.1	60.4
46C-130	7.55	237.6	12.5	55.2	20834.0	77.8	37.3	6.0	1.0
82-30	11.30	1673.1	56.2	25.5	2239.0	ND	0.9	1.7	353.0
82-100	11.64	5297.8	225.6	89.1	34326.0	ND	35.6	50.4	974.0
83C-25	6.98	17.8	1.9	52.2	17658.0	89.2	27.6	6.6	690.0
83C-50	6.96	41.8	6.4	54.9	20633.0	104.0	27.9	5.8	764.0
83C-75	7.81	78.7	20.8	71.5	36871.0	ND	33.9	10.6	772.0
83C-100	9.80	101.8	83.4	38.6	36953.0	ND	27.7	9.3	223.0
83C-130	11.41	2146.3	548.8	143.0	55167.0	ND	42.4	70.8	1392.0

ND-Not detected

In the simulations, pH was varied from 7 to 14 while allowing precipitation of the most soluble solid phase of each element. Variation in total dissolved concentration of these analytes (H_4SiO_4, Al^{+3}, Ca^{+2}, Mg^{+2}) in the solution was analyzed with varying pH. If the predicted concentration vs pH trend for the analyte was not as prominent or in the direction of the observed trend, the next most soluble solid phase containing that analyte was included as a precipitate. Figures 3.1.2.1 to 3.1.2.4 compare model predictions of Si, Al, Ca and Mg levels with the observed concentration trends in the groundwater samples.

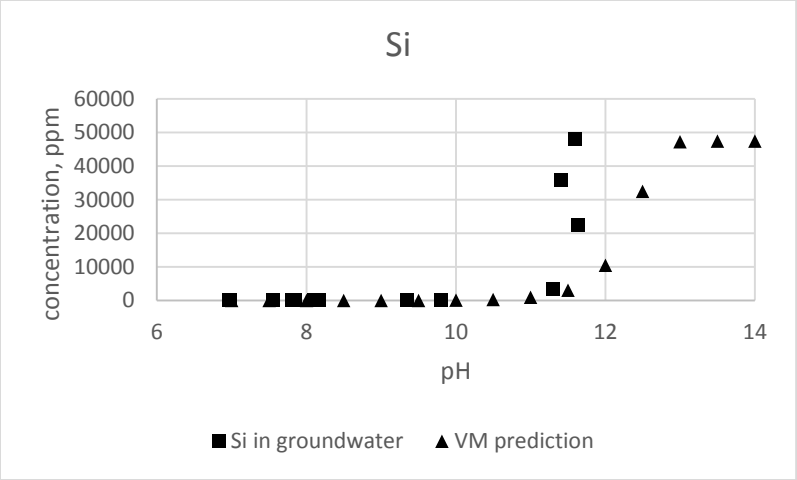

Figure 3.1.2.1 Comparison of Si concentration trends determined for the Oxy site groundwater and predicted using VM modeling

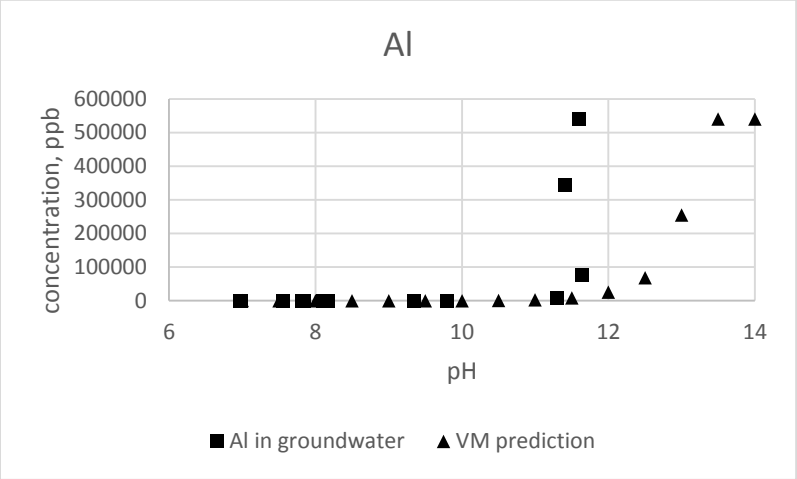

Figure 3.1.2.2 Comparison of Al concentration trends determined for the Oxy site groundwater and predicted using VM modeling

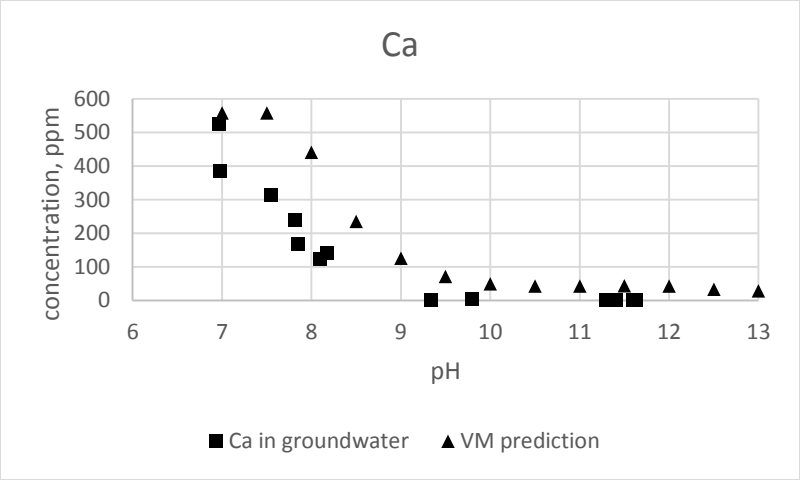

Figure 3.1.2.3 Comparison of Ca concentration trends determined for the Oxy site groundwater and predicted using VM modeling

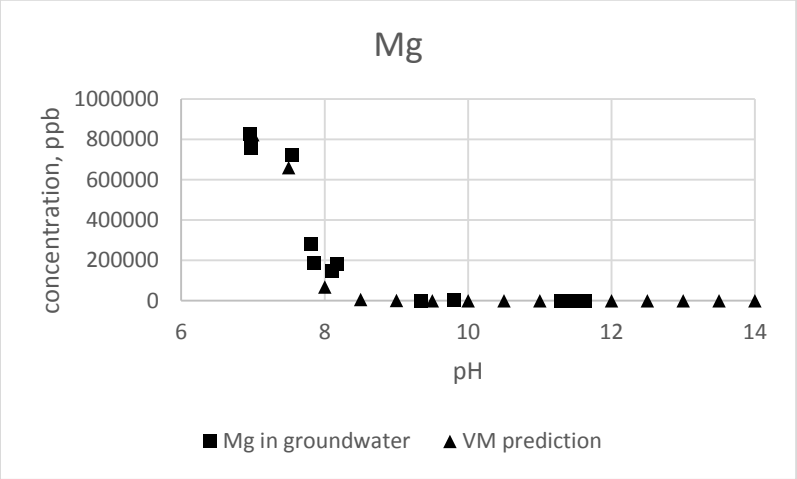

Figure 3.1.2.4 Comparison of Mg concentration trends determined for the Oxy site groundwater and predicted using VM modeling

The VM predicted concentration trends for these elements tend to be comparable with observed trends in groundwater. Characteristically, the model predictions for the dissolution for Si and Al (pH 11 onwards) and precipitation for Ca and Mg (pH 8 onwards) coincide with the groundwater analyses. However, the VM prediction for sensitivity of dissolution (i.e. slope of the curve) is less than that observed, but the prediction for sensitivitiy of precipitation is approximately the same. Model predicted solution phase concentrations of Si and Al at higher pH are less than those measured in the groundwater (Figure 3.1.2.1

and Figure 3.1.2.2). A plausible explanation for this deviation could be the formation of soluble complexes of these species with organic compounds present in the groundwater or their colloidal mobilization. Since, the VM model input did not include organic carbon, that model did not account for possible impacts of those complexes, resulting in lower predicted concentrations of these elements in solution. In addition, the model predicted that $H_3SiO_4^-$ and $H_2SiO_4^{2-}$ were the dominant dissolved Si species at higher pH but upon introduction of pentanuclear Si species, VM predictions for solution phase Si concentrations were closer to groundwater analyses at higher pH. However, Si concentraion trends determined in the groundwater can not be explained by the presence of only one type of Si specie.

In contrast to the prediction made for Si and Al, VM predicted higher concentration of Ca in solution as compared to groundwater, especially at lower pHs (Figure 3.1.2.3). A possible explanation for this could be that VM predicted soluble Ca concentration are based on the precipitation of the specified solid phase only. Whereas in the aquifer conditions, Ca could be precipitating as other solids. Hence, the VM model predicted concentration could be higher than observed concentration in the groundwater.

It should be noted that there are many other factors that could cause the groundwater (extracted from Oxy site) composition to differ from the model prediction, and the above mentioned reasons for this deviation are plausible but not necessarily the correct ones.

3.1.3 Aquatic chemistry of Silica

In aqueous soil solutions, amorphous silica can be present in the form of silicic acid (H_4SiO_4 or $Si(OH)_4$) (Rimstidt, 1997) and/or in the form of polynuclear complexes with varying stoichiometries. These polynuclear Si species can form very large chains.

When considered at its simplest stoichiometry, amorphous SiO_2 dissolves in water following the reaction below:

$$SiO_2 + 2H_2O \rightarrow Si(OH)_4 \qquad \text{eq 3.1.3.1}$$

The soluble silica ($Si(OH)_4$) can deprotonate to form silicate ions. This can also initiate the formation of polynuclear species eventually resulting in the growth of large molecules. This process can be referred to as hydroxide catalyzed anionic polymerization (Amjad and Zuhl, n.d.) as per equation 3.1.3.2.

$Si(OH)_4 + OH^- \rightarrow (HO)_3Si—O^- +$ other silicates

Silicate + $Si(OH)_4 \rightarrow (OH)_3Si\text{-}O\text{-}Si(OH)_3 \rightarrow$Colloidal silica eq 3.1.3.2

If all the Si in the aqueous solution is present as only monomers, its variation in solubility with pH can be explained as presented below.

Silicic acid can donate multiple protons and can undergo the following dissociation reactions (Benjamin, 2014).

$H_4SiO_4 \rightarrow H_3SiO_4^- + H^+$ $pK_{a1} = 9.84$ eq 3.1.3.3

$H_3SiO_4^- \rightarrow H_2SiO_4^{-2} + H^+$ $pK_{a2} = 13.2$ eq 3.1.3.4

Using the above acid dissociation constants, effects of pH on the distribution of silicic acid species can be calculated as shown in Figure 3.1.3.1. At lower pH (pH < 8), protonated specie (H_4SiO_4) is dominant. As pH increases (between pH 10 and 13.2), deprotonated specie ($H_3SiO_4^-$) is dominant and at pH > 13.2, $H_2SiO_4^{2-}$ specie is dominant. Since the solubility of the ionic form (deprotonated specie) is orders of magnitude higher than the neutral specie (Schwarzenbach et al., 2002) and ionic forms are orders of magnitude higher than the neutral specie at high pH, the solubility of Si in water is strongly pH dependent.

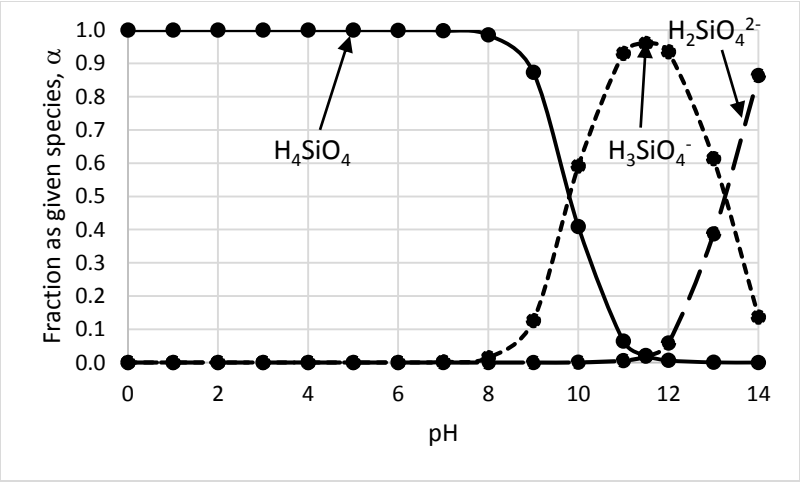

Figure 3.1.3.1 Distribution of Si species as a function of pH

As per the relevant equilibria constants included in the VM database, aqueous solubility of amorphous silica at 25°C and pH 7 is about 103 mg/l which is equivalent to 164.8 mg/l of H_4SiO_4. Aqueous Si

concentrations can be calculated considering this neutral specie solubility and its fractional presence at varying pH. Figure 3.1.3.2 shows exponentially increasing concentrations of Si with increasing pH; this increase is caused, as mentioned above, by the prevalence of anionic forms of silicic acid.

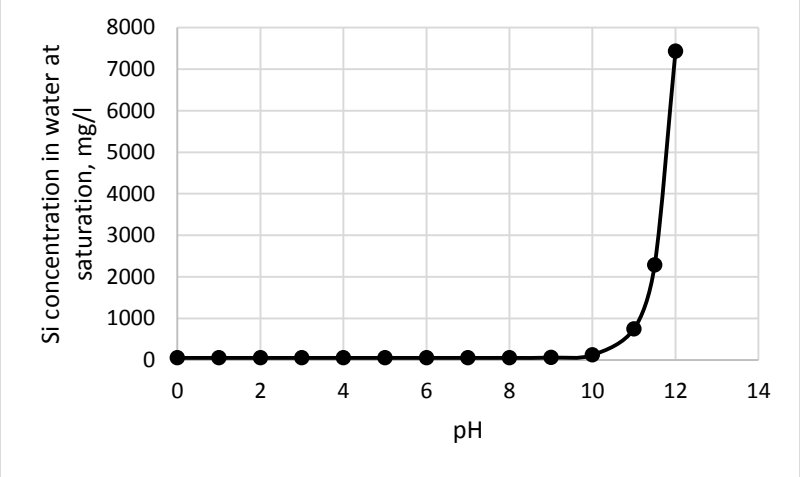

Figure 3.1.3.2 Aqueous Si concentration as a function of pH

Figure 3.1.3.2 partially explains the extremely high concentrations of Si present in groundwater samples e.g. Well #7, 82-100 and 83C-130 (Table 3.1.2.1) with elevated pH (11.4-11.6, Table 3.1.1.1.1). However, the Oxy site groundwater contains a much higher concentration of dissolved Si (48000 ppm at pH 11.6) than that anticipated based on the equilibria of silicic acid only. This indicates the plausible presence of polynuclear or macromolecular complexes of Si and other Si solutes or colloidal species, possibly including those stabilized by organic matter abundant in the Oxy site water.

3.2 Si precipitation from the Oxy site groundwater

The following sections describe visual observations made during Si precipitation by acidification and $CaCl_2$ addition. They also present the concentrations of dissolved Si and percent Si precipitated after each incremental acid/salt addition.

3.2.1 Acid addition

3.2.1.1 Visual Observations

Slow acid addition:

A few white fluffy solids were observed in the sample when the pH was lowered to approximately around pH 11. The flocs were initially about 3-4 mm across and irregular in shape, but continuous stirring broke the solids into smaller units. The concentration of solids significantly increased with each acid addition and the particle size decreased with continued mixing, making the suspension thicker and slower to settle. The solids comprised a major portion of the suspension at the end of acidification, however after a day of settling they occupied only about 40% of the total system volume (Figure 3.2.1.1.1). At that time, the supernatant looked clear (devoid of solids, but still dark colored).

Rapid acid addition:

Precipitation was instantaneous and the voluminous precipitate looked like a gel with very little free water rather than individual particles suspended in a solution (Figure 3.2.1.1.2). The gel formed upon rapid acid addition was impossible to mix.

3.2.1.2 Acid addition experiment results

Continuous acid addition dilutes the groundwater and hence lowers the concentration of total Si (dissolved plus precipitated) in the system. Appendix 2 presents calculation steps followed to estimate the percent groundwater in the system and correct for its dilution. The measured pH and dissolved Si analyzed in the sample collected after each incremental acid addition are shown in Appendix 3.

Figure 3.2.1.1.1 Visual appearance of solids precipitated as a result of slow acid addition to groundwater from Well 82 at 100-ft depth (initial pH: 11.786, Final pH: 9.809)

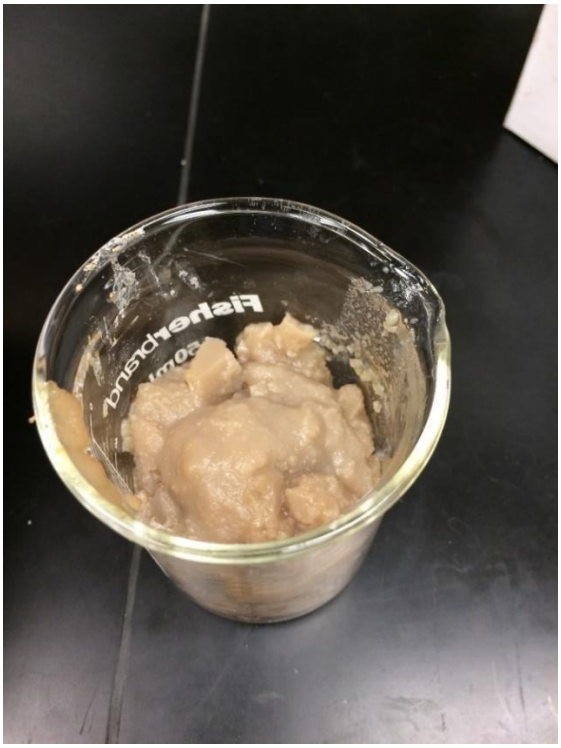

Figure 3.2.1.1.2 Visual appearance of solids precipitated as a result of rapid acid addition to groundwater from Well 82 at 100-ft depth (initial pH: 11.786)

The difference between the total and dissolved Si concentrations after acid addition was assumed to equal the concentration precipitated.

Figure 3.2.1.2.1 shows that increasing amounts of Si precipitate as the pH is decreased. Precipitation started at pH 11, and about 96% of the Si had precipitated when the pH had dropped to 10.5.

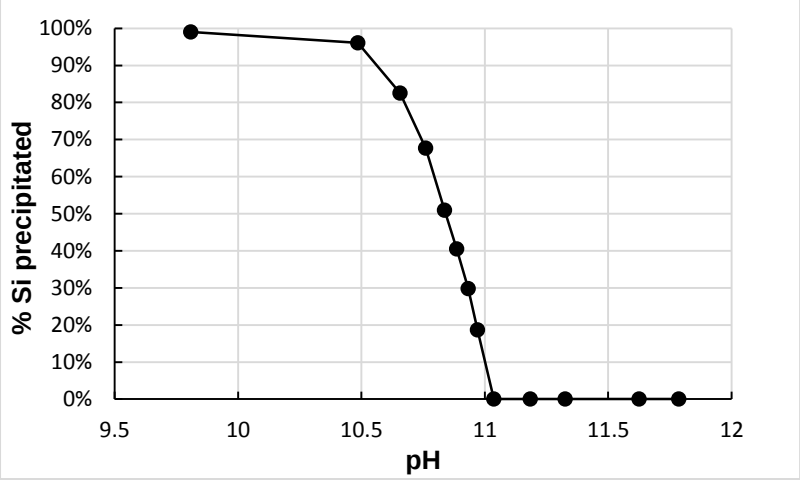

Figure 3.2.1.2.1 Percent Si precipitation with decreasing pH (Groundwater from Well 82 at depth 100-ft)

3.2.2 $CaCl_2$ addition

3.2.2.1 Visual observation

<u>Rapid $CaCl_2$ addition:</u>

Solids precipitation was instantaneous and so voluminous that mixing was impossible; the entire batch of groundwater turned into a thick mass with very little free water (Figure 3.2.2.1.1)

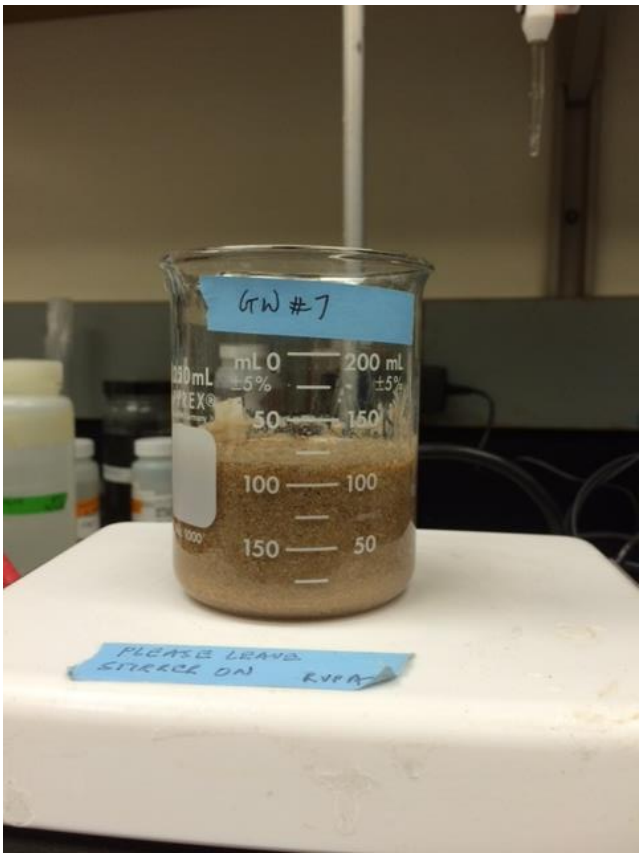

Figure 3.2.2.1.1 Visual appearance of solids precipitated as a result of rapid $CaCl_2$ addition to groundwater from Well 7 at 130-ft depth (initial pH: 11.6)

Slow $CaCl_2$ addition:

Solid flakes were observed floating on the surface as soon as salt was added. The flakes were harder to break than those formed in the acid addition experiment; a higher mixing speed was therefore used to break them into smaller particles. More solids were observed with continued salt addition. Solids comprised a large portion of the suspension at the end of experiment, occupying about 50% of the suspension after a day of settling (Figure 3.2.2.1.2).

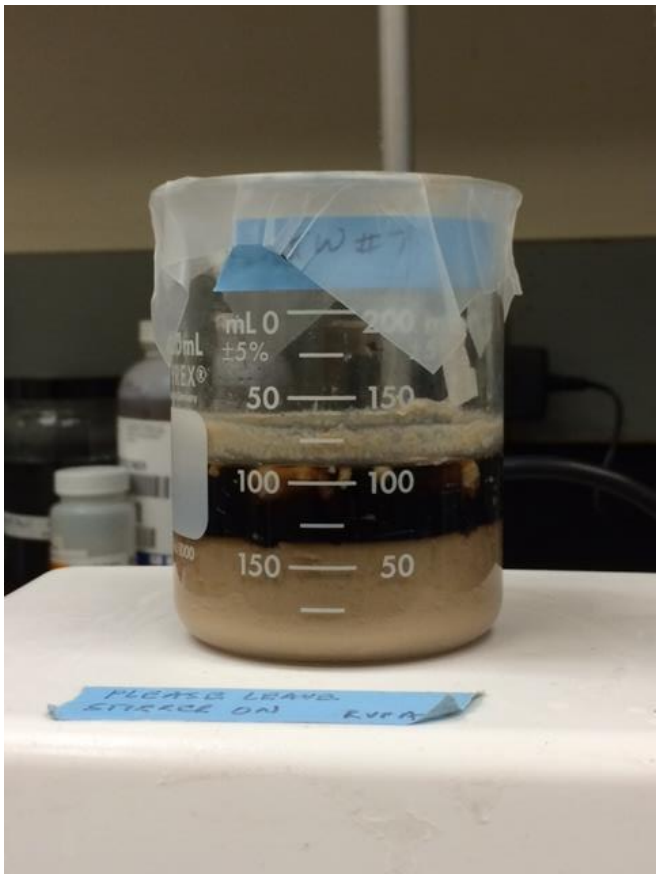

Figure 3.2.2.1.2 Visual appearance of solids precipitated as a result of slow $CaCl_2$ addition to groundwater from Well 7 at 130-ft depth (initial pH: 11.6, Final pH: 11.09)

3.2.2.2 $CaCl_2$ addition experiment results

Appendix 4 shows the dissolved Si concentration and the corresponding percent Si precipitated after each $CaCl_2$ addition. The $CaCl_2$ addition did not dilute the groundwater noticeably, so the percent groundwater was assumed to remain at 100% throughout the experiment. The pH of the suspension was ~11 at the end of the experiment.

Figure 3.2.2.2.1 shows increasing Si precipitation with $CaCl_2$ addition. The percent Si precipitated is linear with $CaCl_2$ addition. About 80% Si was precipitated with 2 g of $CaCl_2$ addition to 100-ml groundwater. If this results are extrapolated, about 2.6 g $CaCl_2$ per 100-ml of groundwater would be required for 100% Si removal.

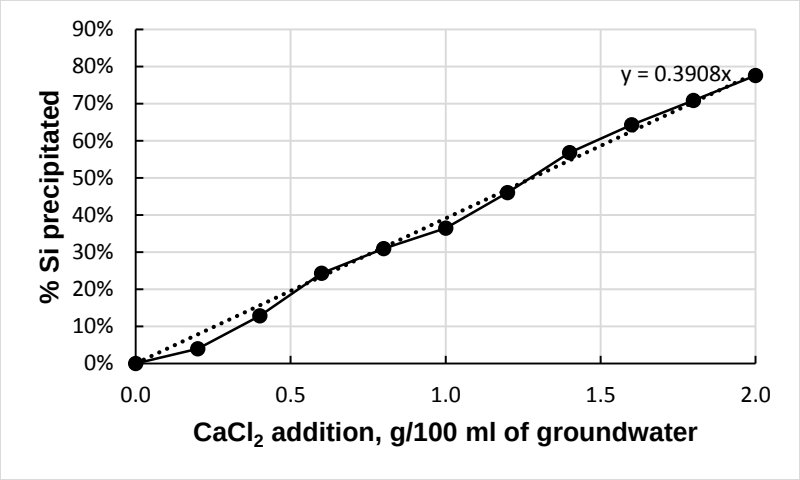

Figure 3.2.2.2.1 Percent Si precipitated as a result of slow $CaCl_2$ addition (Groundwater from Well 7 at depth 130-ft)

3.2.3 Discussion and implication

Visual observations indicated that rapid addition of either $CaCl_2$ or acid to groundwater generates a large volume of solids that require further processing and disposal, whereas slow addition of acid or salt generates a much lower amount of solids (about 40-50%) of total batch volume. Thus, rapid addition of reagents should not be used for Si removal from the groundwater.

It appeared that slow addition of $CaCl_2$ resulted in a marginally larger volume of solids than slower acid addition did. Accordingly, Si precipitation was achieved by slow acid addition in all further experiments that dealt with processing of solids.

In the studied groundwater, almost all (~99%) of the dissolved Si precipitated when pH was lowered to less than 10. Thus, if groundwater with a significant concentration of dissolved Si (>22000 ppm) is adjusted to pH less than 9 during *ex-situ* treatment, precipitation will generate large amounts of solids. The generated solids will require processing to reduce the volume that needs to be handled and disposed of.

3.3 Treatment and processing of solids generated during *ex-situ* treatment of groundwater

The following sections present results and discussion of the approach investigated to reduce the volume of the solids after precipitation.

3.3.1 Precipitation of solids during *ex-situ* treatment

Table 3.3.1.1 presents the yield of wet solids and the fractional removal of Si from the groundwater by acidification. Figure 3.3.1.1 shows the wet precipitated solids.

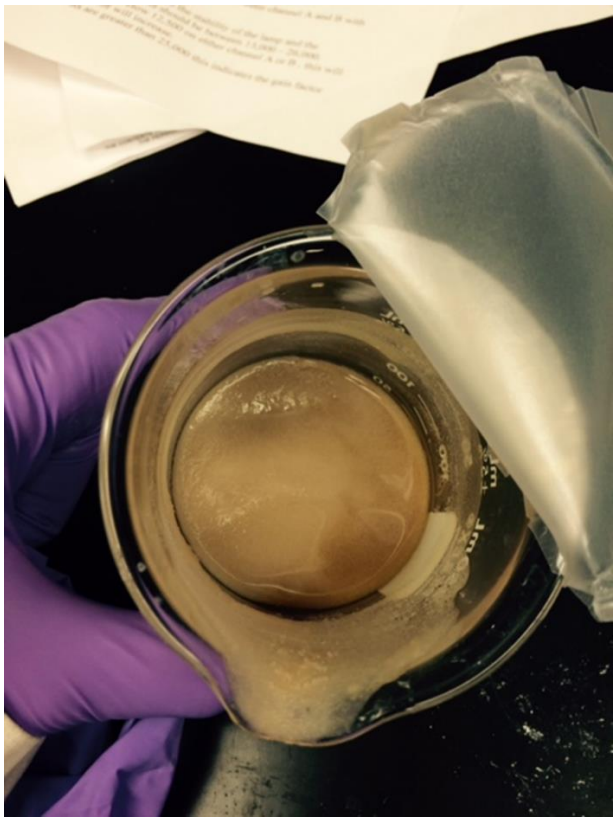

Figure 3.3.1.1 Visual appearance of wet solids collected after decanting the supernatant (Groundwater: Well 82 @ 100-ft depth)

Table 3.3.1.1 Yield of wet solids and Si removal by acidification of groundwater

	Calculation step	Well 7-130	Well 82-100	Well 82-100 (Repeat experiment)
Volume of groundwater, ml		100	100	100
Weight of groundwater, g	A	113.9	108.6	108.6
Volume of HCl added, ml		39	27	27
Weight of batch after HCl addition, g	B	151.2	133.0	134.2
Volume of solids (Visual observation), % of batch volume		33% (after 6 d of settling)	40% (after 1 d settling)	Data not available
Supernatant decanted, g	C	100.6	86.2	91.5
Weight of wet solids, g	D = B-C	50.7	46.8	42.7
% yield of wet solids based on groundwater weight	E = D/A	44.5%	43.1%	39.3%
% Si precipitation				ND
Dissolved Si in raw groundwater, ppm		40108	21691	
Dissolved Si in supernatant, ppm		141	106	
% groundwater in system after acidification (Ref: Appendix 2)		72%	78.7%	
% Si precipitation (Ref: Appendix 3)		99.5%	99.4%	

ND: Not determined

3.3.2 Mechanical squeezing (dewatering) of wet solids

The yield of dewatered solids and the associated calculations are shown in Table 3.3.2.1. Figure 3.3.2.1 shows the dewatered solids generated from Well 82 groundwater at depth 100-ft.

Table 3.3.2.1: Yield of dewatered solids generated from mechanical squeezing of the wet solids

	Calculation step	Well 7-130	Well 82-100	Well 82-100 (Repeat experiment)
Weight of wet solids squeezed, g	F	7.8	12.8	18.2
Weight of dewatered solids, g	G	3.4	4.8	7.1
% weight reduction by dewatering	(F-G) / F	56.3%	62.5%	61.3%
Weight of dewatered solids (if applied to entire batch of wet solids), g	H = (D/F) * G	22.1	17.6	16.6
% yield of dewatered solids based on groundwater weight	H/A	19.4%	16.2%	15.2%

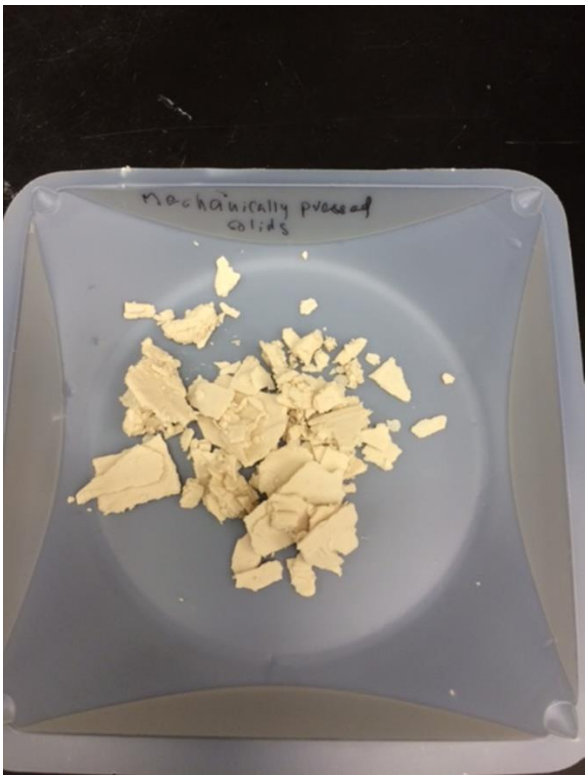

Figure 3.3.2.1 Visual appearance of dewatered solids (Groundwater: Well 82 @ 100-ft depth)

Table 3.3.2.2 summarizes the major components analyzed in dewatered solids.

Table 3.3.2.2 Composition of the dewatered solids

	Calculation step	Well 7-130	Well 82-100	Well 82-100 (repeat experiment)
Weight of dewatered solids dissolved, g	I	0.1605	0.0932	0.1706
Volume of solution prepared, ml	J	0.5449	0.2808	0.5491
Dissolved Si analyzed in solution using ICP-MS, ppm	K	52856	53381	44521
Dissolved Ca analyzed in solution using ICP-MS, ppm	L	ND	ND	712.6
Si in solution prepared, g	M = ((K/1000)*J)/1000	0.0288	0.0150	0.0244
Ca in solution prepared, mg	N = ((L/1000)*J)/1000	ND	ND	0.39
% Si in solids	M/I	17.9%	16.1%	14.3%
% Ca in solids	N/I	ND	ND	0.2%

ND: Not determined

3.3.3 TGA of dewatered solids and drying at selected temperature

Figures 3.3.3.1 and 3.3.3.2 show TGA results for the dewatered solids.

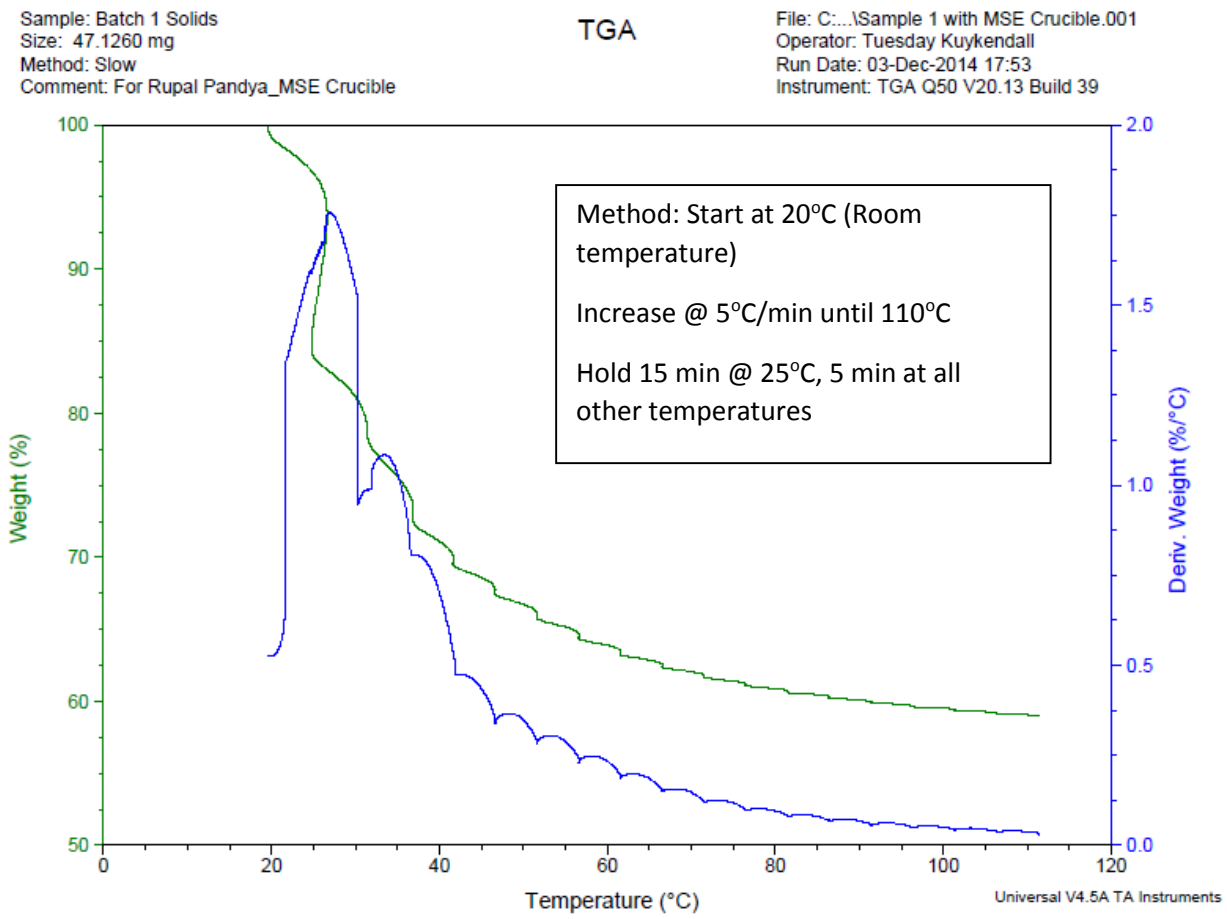

Figure 3.3.3.1 TGA result of dewatered solids generated from Well 7 groundwater at depth 130-ft

The TGA results for the dewatered solids generated as a result of treatment of Well 7 groundwater (Figure 3.3.3.1) showed that the sample lost about 30% of its weight when it was dried at temperatures <40°C and that the solids lost an additional 10% of their weight when the temperature was increased to 110°C. The rate of decrease of weight was maximal in the temperature range of 20-40°C. These results suggest that most of the benefits of drying can be achieved by heating the solids to between 20-40°C.

Based on these results, in the next run of TGA analyses of dewatered solids, the sample was held at 30°C for about an hour.

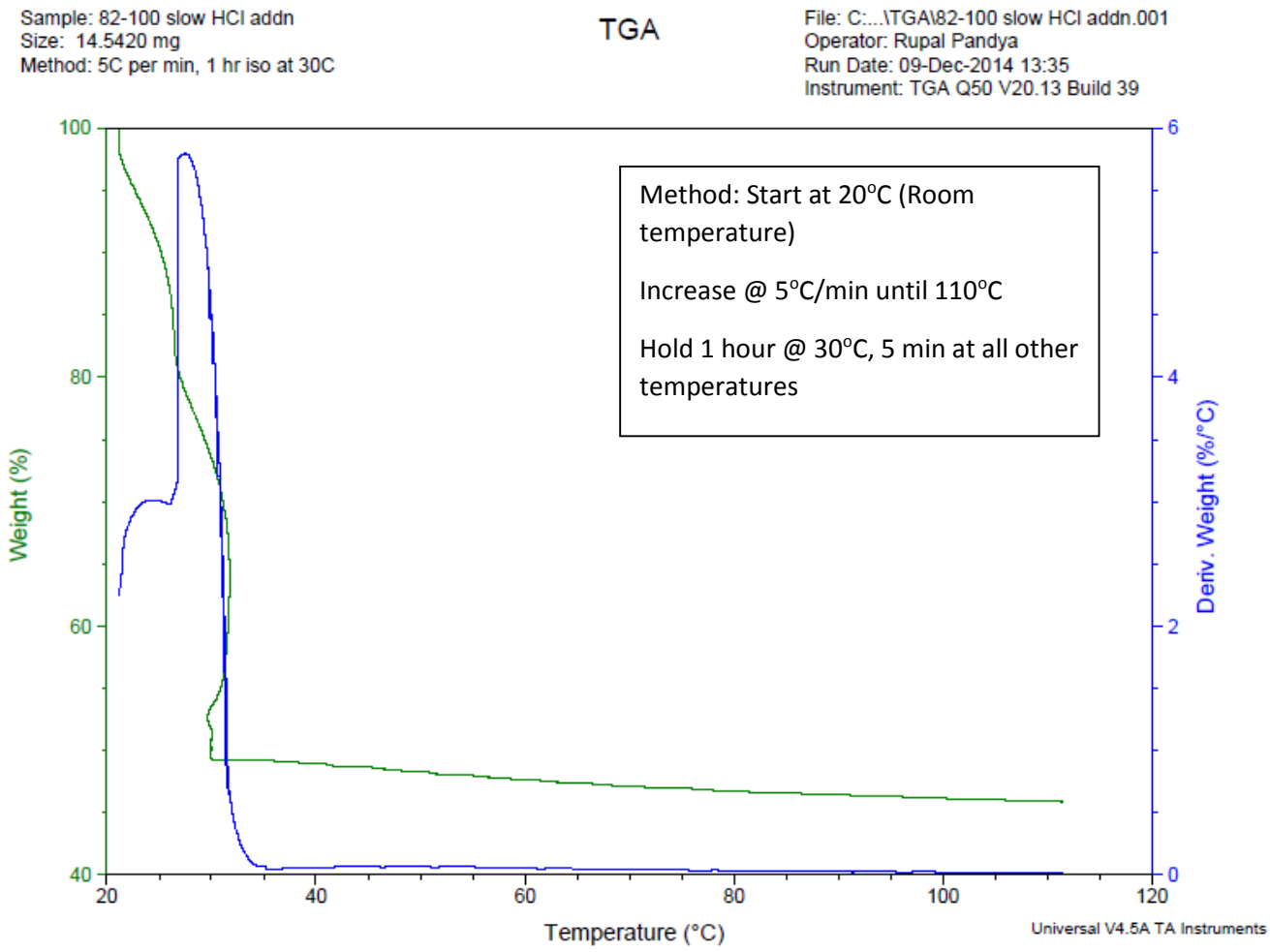

Figure 3.3.3.2 TGA result of dewatered solids generated from Well 82 groundwater at depth 100-ft

The sample had lost more than 50% of its weight at the end of the isothermal period at 30°C, and it lost an additional ~5% of its weight upon further increase of temperature (Figure 3.3.3.2).

Based on these data, a drying temperature of 30°C was chosen. The composition of solids dried at this temperature is summarized in Table 3.3.3.1. Figure 3.3.3.3 shows the dried solids.

Table 3.3.3.1 Percent yield of dried solids after drying the dewatered solids at T=30°C for about 24 hours

	Calculation step	Well 82-100
Weight of dewatered solids, g	O	7.057
Weight of dried solids, g	P	3.093
% Weight reduction by drying	(O-P)/O	56.2%
Weight of dried solids (if applied to entire batch of dewatered solids), g	Q=(H/O)*P	7.3
% yield of dried solids based on groundwater weight	Q/A	6.7%

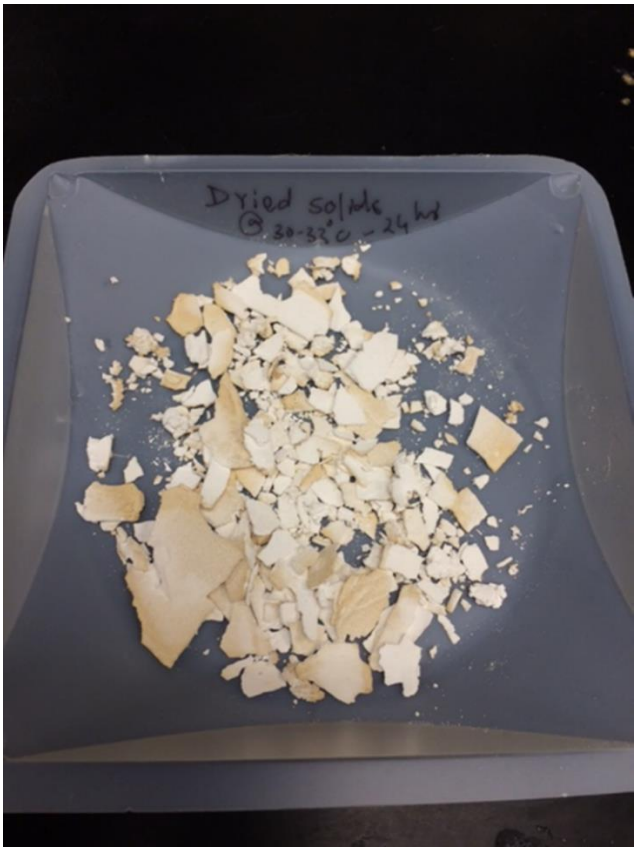

Figure 3.3.3.3 Visual appearance of dried solids (Well 82 groundwater @ 100-ft depth)

The dried solids were friable and thus were easily ground into a powder. Such a powder was generated (Figure 3.3.3.4) and was used to fill a 2-ml vial. The volume occupied by 1.0 g of the powder was 2.17-ml (that is their packed density was 2.17 g/cm^3). Thus, applying this value to the entire batch (7.3 g, Ref Table 3.3.3.1) of dried solids generated, the volume of dried solids would be 15.9 cm^3.

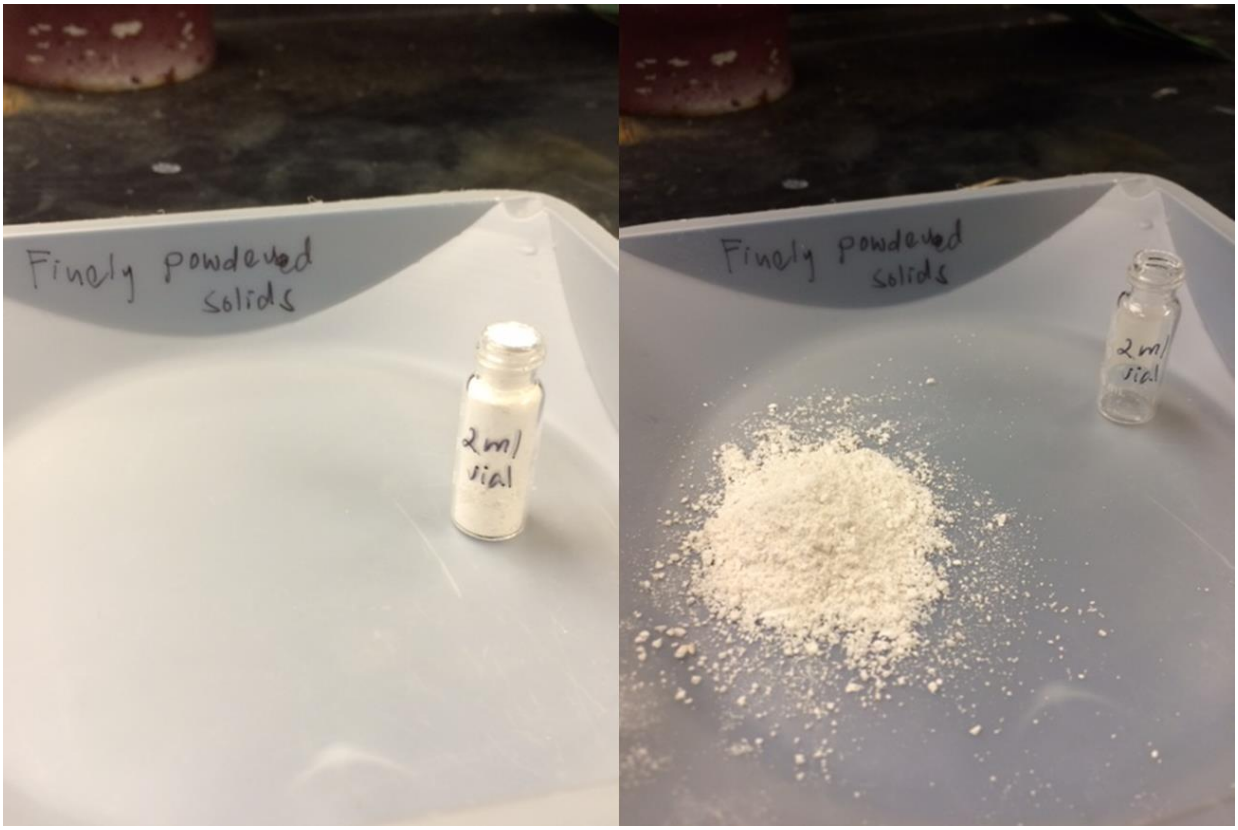

Figure 3.3.3.4 Visual appearance of finely ground powdered dried solids placed in 2-ml vial

Table 3.3.3.2 shows the concentrations of Si, Al, and Ca in the dried solids.

Table 3.3.3.2 Major contents analyzed in dried solids generated by 24 hours drying at T = 30°C

	Calculation step	Well 7-130	Well 82-100 (Repeat experiment)
Weight of dried solids dissolved, g	R	0.1199	0.1141
Volume of solution prepared, ml	S	0.695	0.706
Dissolved Si analyzed in solution, ppm	T	64691.7	63831
Dissolved Ca analyzed in solution, ppm	U	769	870.5
Dissolved Al analyzed in solution, ppm	V	740.5	163
Si in solution prepared, mg	W = ((T/1000)*S)/1000	44.96	45.1
Ca in solution prepared, mg	X = ((U/1000)*S)/1000	0.53	0.61
Al in solution prepared, mg	Y = ((V/1000)*S)/1000	0.515	0.115
% Si in solids	W/R	37.5%	39.5%
% Ca in solids	X/R	0.4%	0.5%
% Al in solids	Y/R	0.4%	0.1%

3.3.4 Discussion and implication

Table 3.3.1.1 indicated that more than 99% of the dissolved Si in the groundwater precipitates when the groundwater pH is lowered to <10. TGA results reinforce the inference that 30°C is an effective drying temperature.

Next, a batch of dewatered solids was dried at 30°C for about 24 hours, causing them to lose 56.2% of their weight. Thus the extension of the drying time (24 hours against 1 hour) did not result in significant reduction in weight. Grinding the dried solids to a fine powder reduces their volume to about 16% of the volume of original untreated groundwater.

Based on the above calculations, a hypothetical scenario can be envisioned in which Well 82 groundwater extracted at 100-ft depth is treated at the rate of 10000 gal/d, and the generated solids are dewatered and dried as per the procedure described. The volume of dried solids that would be generated and would require disposal is

$$10{,}000\ \frac{gal}{d} * 3.78\ \frac{L}{gal} * 0.16\ \frac{L\ of\ dried\ solids}{L\ of\ groundwater} * \frac{1\ ft^3}{28.3\ L} = 213\ \frac{ft^3 of\ solids}{d}$$

The elemental analyses of the dried solids (Table 3.3.3.2) indicated that the dried solids contain about 38.5% of Si by mass.

The experiment results demonstrate reasonable reproducibility of the results from three different experiments. This confirms the technical viability of the process. However its economic viability needs to be assessed.

Presuming the Si present in the solids is in the form of SiO_2, the dried solids generated from the described *ex-situ* treatment of the groundwater are about 82% SiO_2 with the remainder of the mass presumably attributable to some remaining embedded water and perhaps some other elements from the original groundwater. These dried solids could have a potential reuse application in cement production.

3.4 Stability of solids

The following sections present results from the dissolution experiment to study stability of the solids.

3.4.1 Results

Figure 3.4.1.1 shows the dissolved Si concentration as a function of pH when three differently aged solids were dissolved. This figure also shows the dissolved Si concentration when pH was reduced during precipitation.

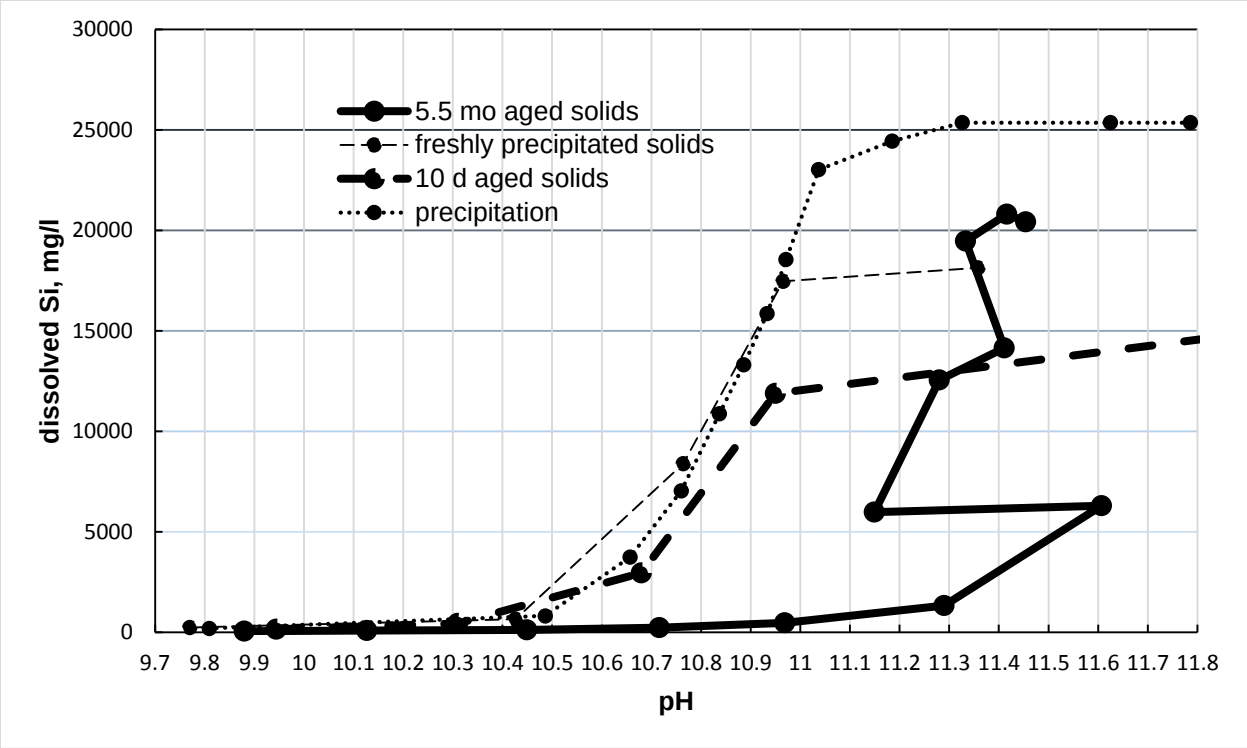

Figure 3.4.1.1 Comparison of dissolved Si concentration (during dissolution and precipitation) as a function of pH

3.4.2 Discussion and implication

The freshly precipitated solids dissolved rapidly as the pH was increased. This experiments result in approximately the same Si concentration vs pH trend as that determined in the experiment in which the acid was added to cause the precipitation of Si based solids. These solids were completely dissolved when the pH was raised to about 11, which is again consistent with the pH at which first precipitation was observed (Figure 3.2.1.2.1). This indicates that the freshly precipitated solids dissolved readily and rapidly.

The solids that had aged for 10 days showed only a slightly increased resistance to dissolution, and the effect of a week-long ageing does not appear to have any practical significance. Still, to achieve a given amount of dissolved Si concentration, the pH of the suspension had to be approximately 0.1 unit higher for 10 days aged solids than that for freshly precipitated solids.

However, 5.5 months aged solids showed a higher resistance to dissolution. The pH of the suspension needed to be raised approximately 0.4 and 0.3 units higher than the freshly precipitated solids and 10

days aged solids respectively, for the same concentration of the Si to dissolve. These solids were completely dissolved around the pH 11.3.

These results indicate that the solids become progressively more chemically stable as they age. This outcome can be very important and necessary to take into account in further work on the examination of formation and stability of Si-containing solids that are intentionally precipitated *in-situ* as a part of remediation approaches to be used to remediate the Oxy site.

3.5 Hydraulic barrier formation and stability

The following section presents results from experiment to study hydraulic barrier formation and its stability.

3.5.1 Batch experiment results

The threshold volumetric proportion of 1 mol/L $NaHCO_3$ to Well 7 groundwater was found to be 1:4. When $NaHCO_3$ solution and Well 7 groundwater were mixed in this ratio, a significant amount of precipitate formed, whereas when they were mixed in a 1:9 ratio, no precipitation was apparent.

3.5.2 Hydraulic barrier formation

Figure 3.5.2.1 shows the inside of the ceramic tube after about 3.5 hour of 1 mol/L $NaHCO_3$ injection. The picture shows the presence of a significant amount of precipitate near the outlet of the tube. This result appears to indicate a non-uniform distribution $NaHCO_3$ solution which preferentially followed the path of least resistance.

To facilitate the mixing of the two solutions as they passed through the soil and with the goal of uniform hydraulic barrier generation in the soil column, two ceramic tubes filled with the unaffected soil (from Well 46 at depth 49-ft) were connected in series (Figure 3.5.2.2). The shell side of the first tube received the $NaHCO_3$ solution whereas, shell side of the downstream tube did not receive any injection. Figure 3.5.2.3 shows the pressure profile that developed following the injection of 1 mol/L and 0.2 mol/L $NaHCO_3$ in separate experiments. Injection of 1 mol/L $NaHCO_3$ solution resulted in rapid increase of pressure drop (up to 31psi) within 30 minutes of groundwater injection as compared to gradual increase in pressure drop (up to 10psi) at the end of 4 hour of 0.2 mol/L $NaHCO_3$ injection.

Figure 3.5.2.1 Inside view of the ceramic tube at the end of 3.5 hour injection of 1 mol/L $NaHCO_3$ solution in Well 7 groundwater passing through unaffected soil from Well 46 at depth 49-ft: Well 7 groundwater @ flow rate = 1.9 ml/min; 1 mol/L NaHCO3@ flow rate = 0.47 ml/min; Darcy velocity: 2.4 cm/min; Unaffected soil from Well 46C at depth 49-ft

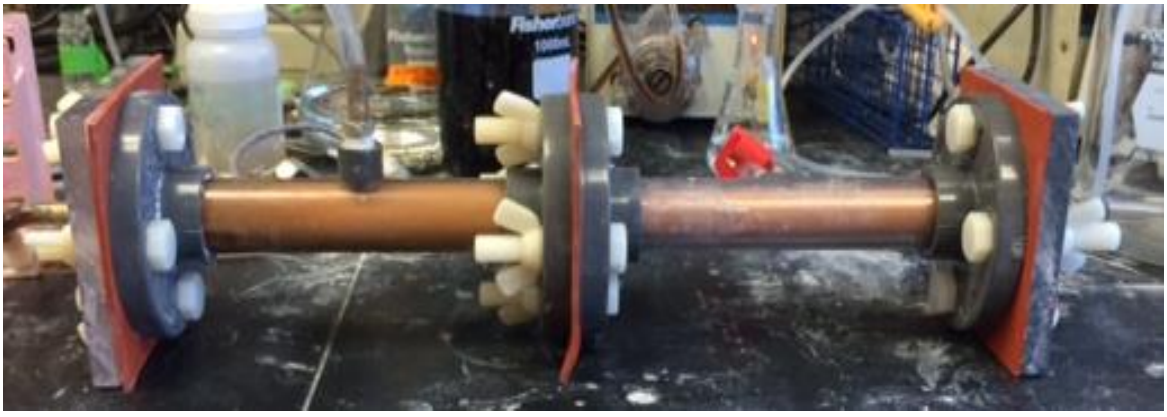

Figure 3.5.2.2 Experiment setup with two columns connected in series

Figure 3.5.2.4 a & b show the inside of both the ceramic tubes at the end of these experiments. They show that the solids had accumulated at the downstream end of the first column or at the inlet of the second column. Because the solids did not migrate or distribute uniformly in the downstream column, the setup was simplified back to the original design with only one soil column in next experiment.

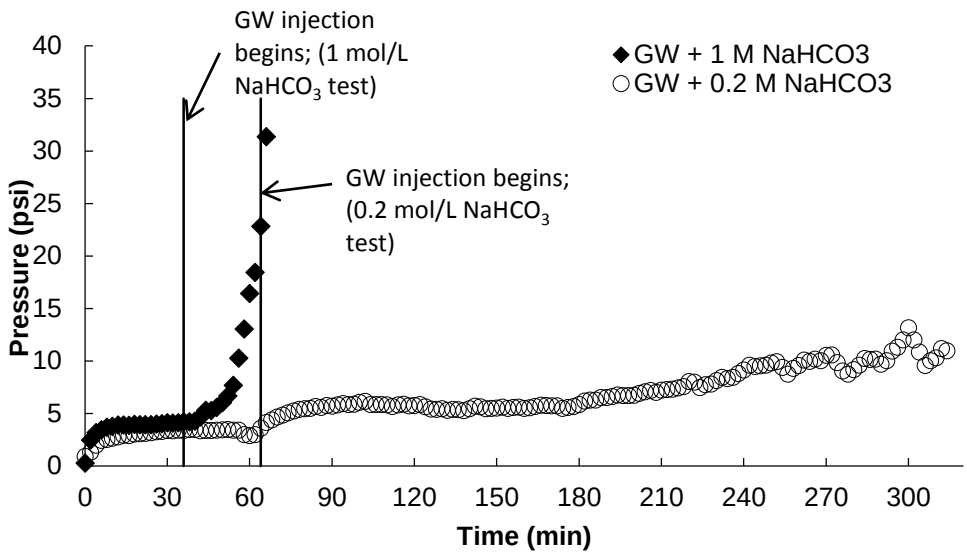

Figure 3.5.2.3 Pressure profile developed after the injection of 1 mol/L $NaHCO_3$ and 0.2 mol/L $NaHCO_3$ solution: Two columns connected in series; Well 7 groundwater @ flow rate = 2 ml/min; 1M / 0.2M $NaHCO_3$@ flow rate = 0.6 ml/min; Darcy velocity: 2.4 cm/min; Unaffected soil from Well 46C at depth 49-ft

Figure 3.5.2.4 a

Figure 3.5.2.4 b

Figure 3.5.2.4 a & b Inside view of both the ceramic tubes at the end of injection of 1 mol/L and 0.2 mol/L $NaHCO_3$ solution in Well 7 groundwater passing through unaffected soil from Well 46 at depth 49-ft

The next experiment involved the injection of 0.4 mol/L $NaHCO_3$ solution for about 8 hours to determine if a longer period of injection would result in hydraulic barrier formation. It was followed by the injection of 1mol/L $NaHCO_3$ solution. Figure 3.5.2.5 shows that even a longer period of injection for 0.4 mol/L $NaHCO_3$ did not result in significant pressure drop, but a dramatic increase in pressure drop was observed as a result of the injection of 1 mol/L $NaHCO_3$. After the formation of a hydraulic barrier i.e. after the pressure drop increased to 17 psi, both the feed solutions were switched to benign solution of pH up to 12.5 to see if the precipitated solids dissolved upon contact with high pH, low Si groundwater. With the limitation of the experiment setup, there was no sign of pressure reversal. However, a longer contact time could dissolve the precipitation or it is also possible that the basicity of the benign solution was being neutralized by much stronger 1 mol/L $NaHCO_3$ that was injected earlier.

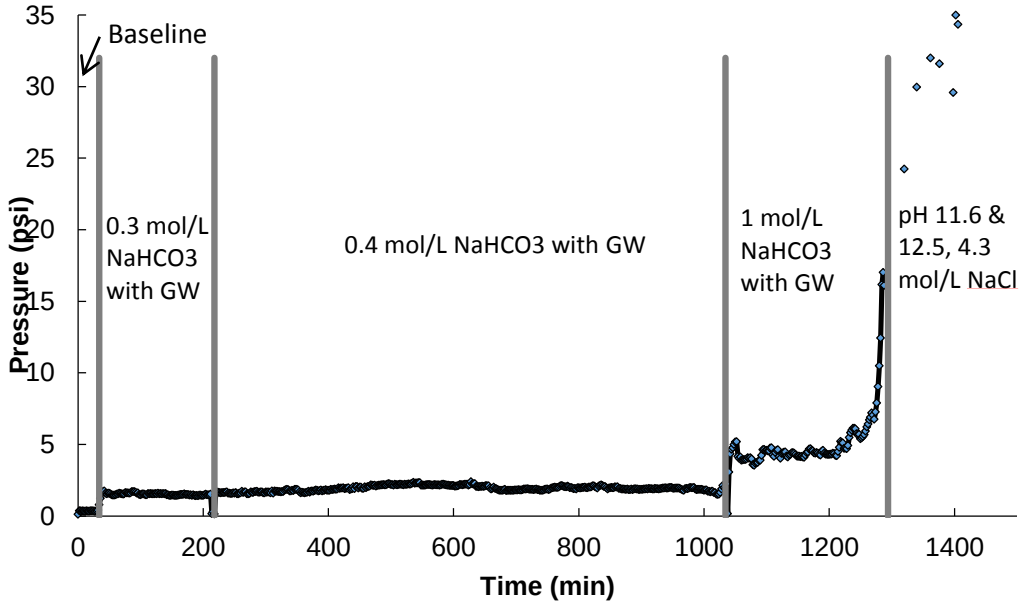

Figure 3.5.2.5 Pressure profile developed after the injection of 0.4 mol/L $NaHCO_3$ followed by 1 mol/L $NaHCO_3$ solution: Well 7 groundwater @ flow rate = 2 ml/min; $NaHCO_3$ flow rate = 0.6 ml/min; Darcy velocity: 2.4 cm/min; Unaffected soil from Well 46C at depth 49-ft

3.5.3 Discussion and next steps

Injection of 1 mol/L $NaHCO_3$ solution in Well 7 groundwater consistently resulted in rapid increase of the pressure drop, whereas even a longer period of 0.4 mol/L $NaHCO_3$ injection did not generate enough precipitates to increase the pressure drop. If we estimate the equivalent H^+ concentration to groundwater ratio at both the concentrations, it is only (0.6 *0.4 /2 =)12 meq/ml of groundwater at 0.4 mol/L $NaHCO_3$ concentration vs 30 meq/ml of groundwater at 1 mol/L $NaHCO_3$ concentration, which is consistent with the observations in batch experiments where 1:9 volumetric ratio of 1 mol/L $NaHCO_3$ to Well 7 groundwater did not result in any precipitation whereas, 1:4 ratio resulted in significant precipitation. This result suggests that a threshold H^+ ion concentration might be required for significant precipitation to occur and for formation of the hydraulic barrier.

Formation of hydraulic barrier and studying its stability are underway to explore whether similar hydraulic barrier formation will take place at different site location where groundwater and soil conditions are different.

Chapter 4 Conclusions and next steps

The maximum concentration of dissolved Si among all the Oxy site groundwater was determined to be about 48000 ppm, which was significantly higher than that anticipated based on relevant chemical equilibria of silicic acid. This provides a strong indication of the plausible presence of polynuclear to macromolecular complexes of Si and other Si solutes stabilized by organic matter. Acidification of the groundwater to pH less than 10 resulted in the removal of almost all the dissolved Si. These experiments also demonstrated that large amounts of solids will be generated if this high pH, high Si groundwater is adjusted to pH less than 9 before discharge. In addition, almost all the Si precipitates within 0.5-0.6 unit drop in pH. Thus, a little change in pH could result in significant amount of precipitation.

If such a high pH, high Si groundwater is to be treated on surface, the resulting solids can possibly be treated by dewatering and gentle drying, producing about 16% (by volume of groundwater) dried solids. The dried solids are about 82% SiO_2 and thus have a potential to be used in cement industry or in related applications. However, the *ex-situ* treatment is contingent upon successful long term extraction of high pH, high Si groundwater, which has been observed to foul the wells because of *in-situ* precipitation.

The phenomenon of heavy precipitation of Si-based solids upon the acidification or other treatment (e.g. addition of $CaCl_2$) of the groundwater can also be utilized to form a hydraulic barrier in the aquifer. Such barriers formed via the *in-situ* precipitation could come in contact with high pH, low Si groundwater. To examine their stability and permeability, extensive enough dissolution experiment are suggested to further ascertain effects of ageing as it seems to increase the resistance of the precipitated solids towards dissolution at high pHs. Experiments related to hydraulic barrier formation points to the requirement of a threshold H^+ ion concentration for significant precipitation to form the hydraulic barrier. The focus of the next phase research is suggested to be on the study of the *in-situ* precipitation and its effectiveness as a barrier for the movement of the Oxy site groundwater. However, it should be noted that the results from laboratory scale experiments are difficult to scale up to aquifer conditions, hence pilot tests are recommended to test the applicability.

References

Amjad, Z., Zuhl, R., n.d. Factors impacting Silica-Silicate Control Agent Performance in Industrial Water Systems.

Benjamin, M.M., 2014. Water Chemistry, 2nd ed. Waveland Press, Inc.

ELAN Software Reference Guide, 2008.

Gorrepati, E., Wongthahan, P., Raha, S., Fogler, H.S., 2010. Si Precipitation in Acidic Solutions: Mechanism, pH effect, and salt effect. Langmuir Artic. 26, 10467–10474. doi:10.1021/la904685x

Inductively Coupled Plasma Mass Spectrometry, EPA Method 6020a, 2007.

Project Plan, University of Washington Kd and pH/Si precipitation testing, 2014.

Remediation System Evaluation, Former Occidental Facility, Tacoma, WA, 2004.

Rimstidt, J.D., 1997. Quartz solubility at low temperatures. Geochim. Cosmochim. Acta 61, 2553–2558. doi:10.1016/S0016-7037(97)00103-8

Schwarzenbach, R.P., Gschwend, P.M., Imboden, Dieter M., 2002. Environmental Organic Chemistry, 2nd ed. Wiley-Interscience.

Tan, S., Horlick, G., 1987. Matrix-effect observations in inductively-coupled plasma mass spectrometry. J. Anal. At. Spectrom. 2, 745–763. doi:10.1039/ja9870200745

Appendix 1 ICP-MS Analytical data for analytes – calibration curve, drift and recovery estimation

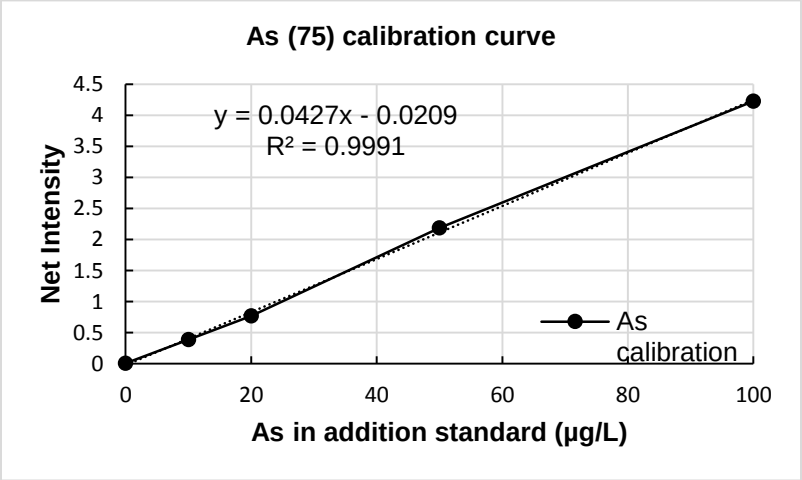

Instrument sensitivity drift for As

= (0.0425 - 0.0427) / 0.0427

= -0.47 %

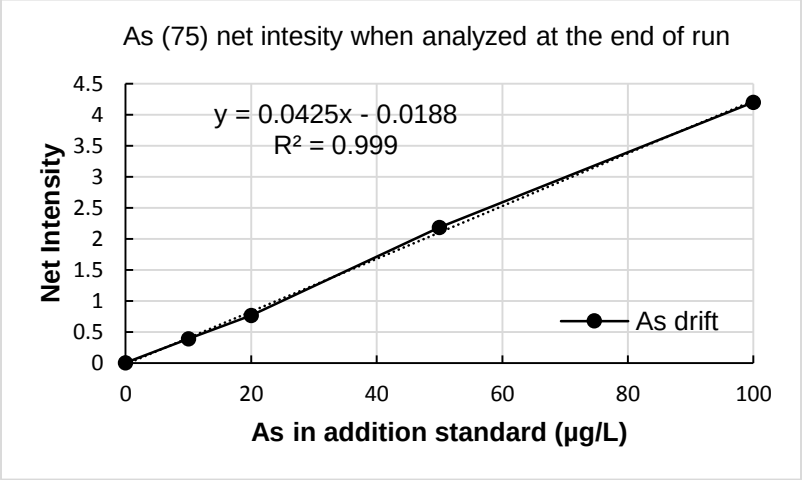

As recovery

= 99.4%

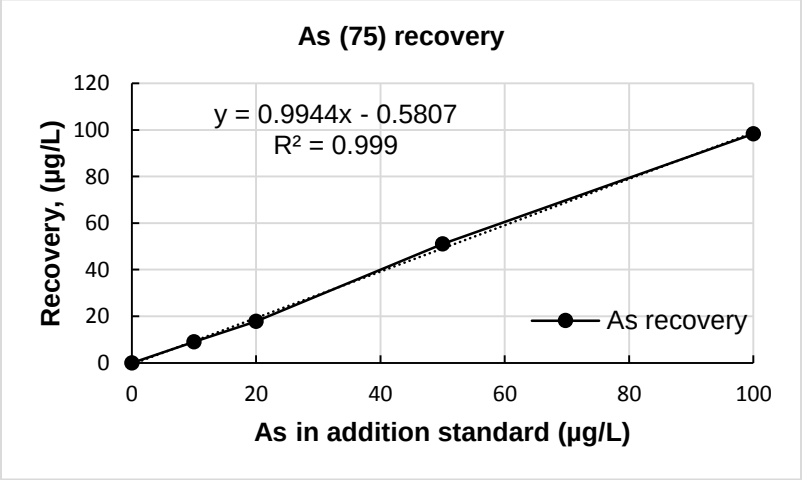

As (75) ICP-MS analytical data: calibration curve, drift and recovery estimation

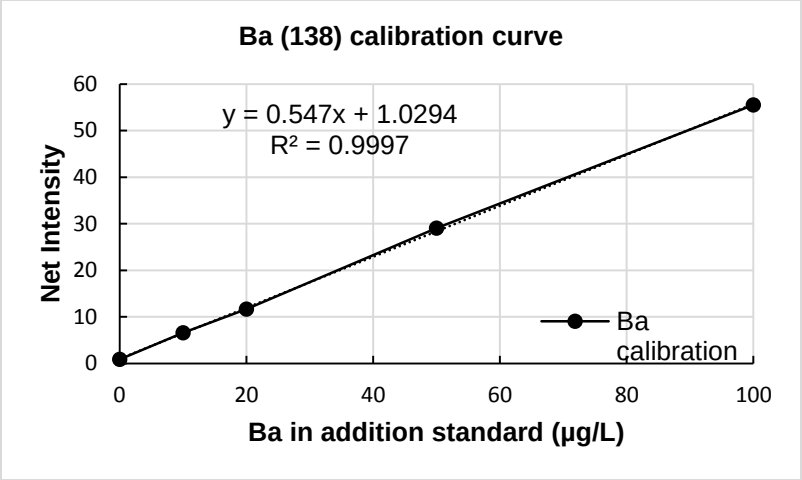

Instrument sensitivity drift for Ba

= (0.6074 - 0.547) / 0.547

= 11.04%

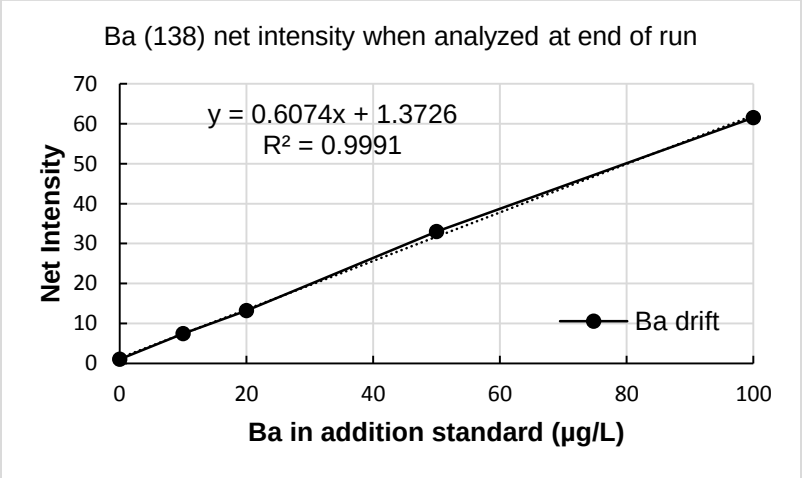

Ba recovery

= 111.0 %

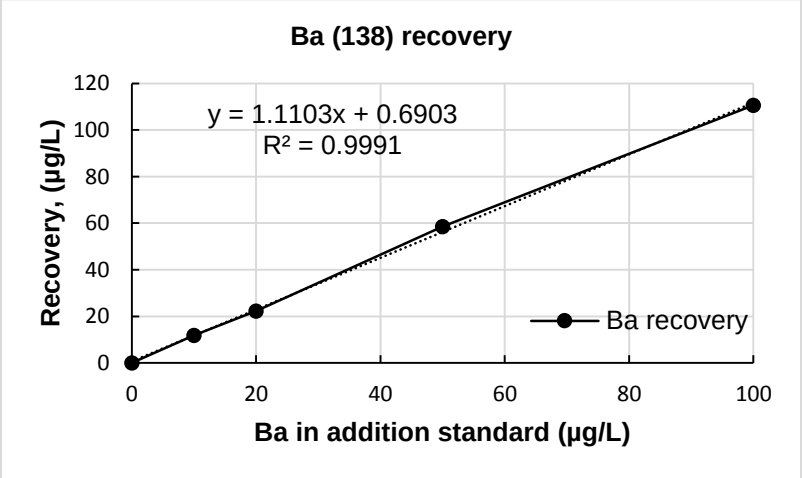

Ba (138) ICP-MS analytical data: calibration curve, drift and recovery estimation

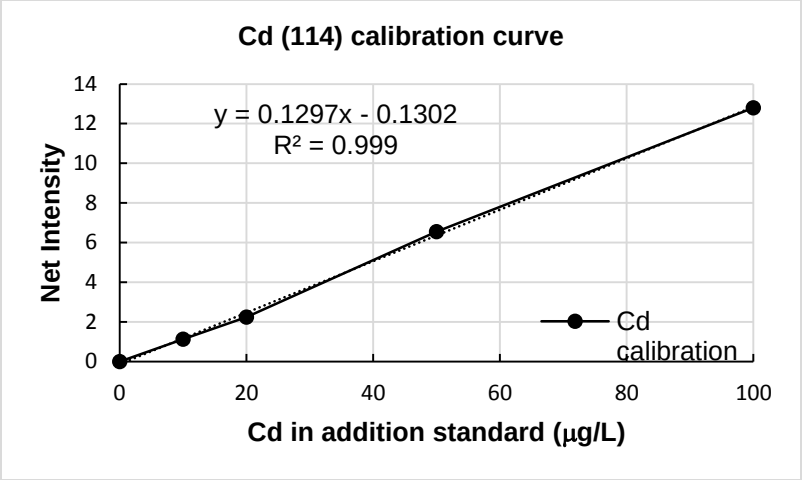

Instrument sensitivity drift for Cd

= (0.1378 – 0.1297) / 0.1297

=6.25%

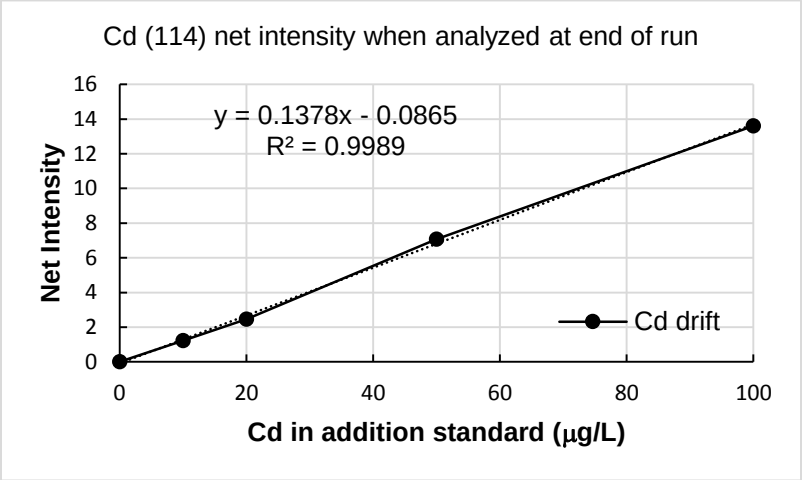

Cd recovery

= 106.2 %

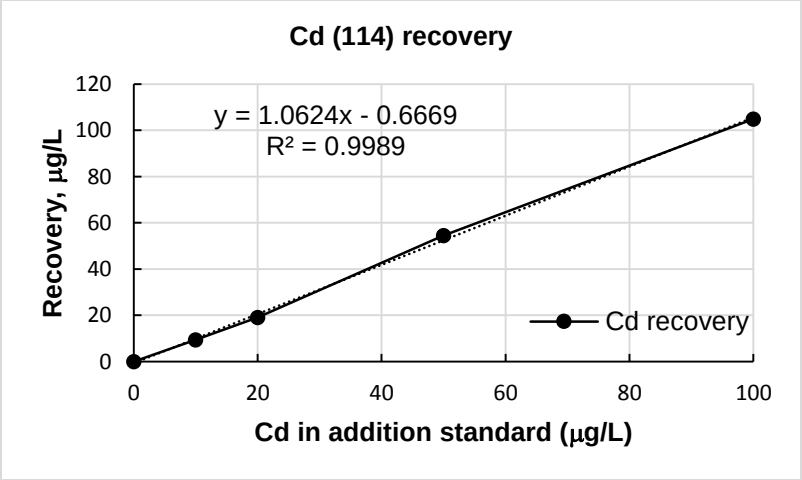

Cd (114) ICP-MS analytical data: calibration curve, drift and recovery estimation

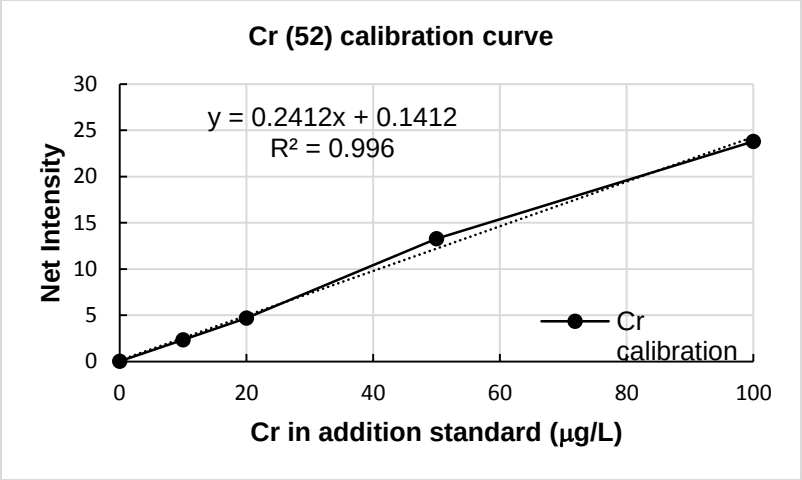

Instrument sensitivity drift for Cr

= (0.2492 – 0.2412) / 0.2412

= 3.32%

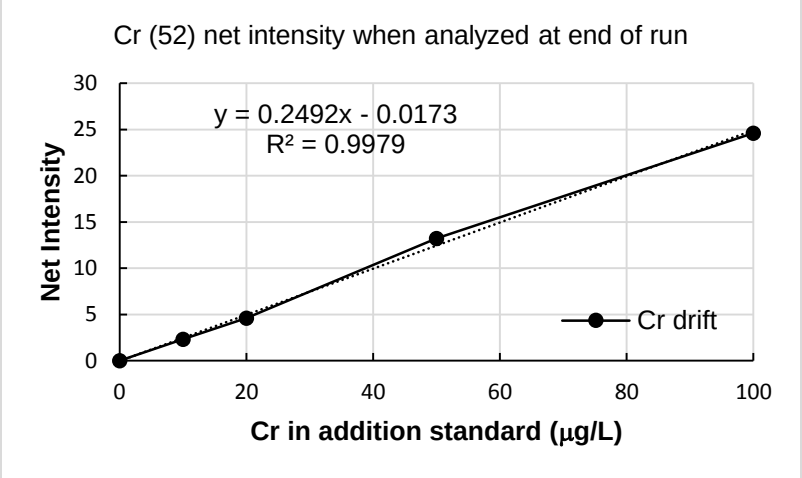

Cr recovery

= 103.3%

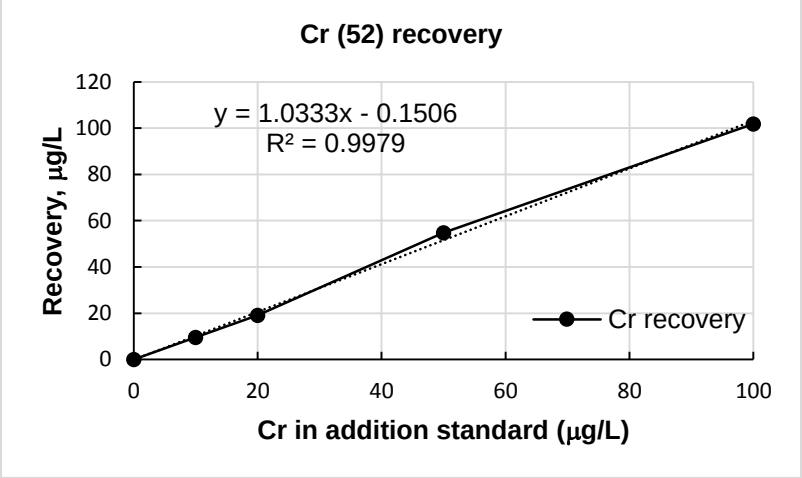

Cr (52) ICP-MS analytical data: calibration curve, drift and recovery estimation

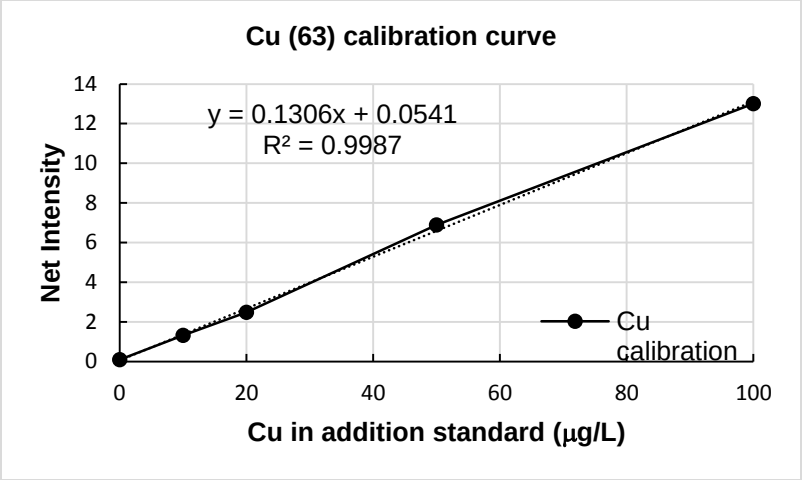

Instrument sensitivity drift for Cu

= (0.1337 – 0.1306) / 0.1306

= 2.37 %

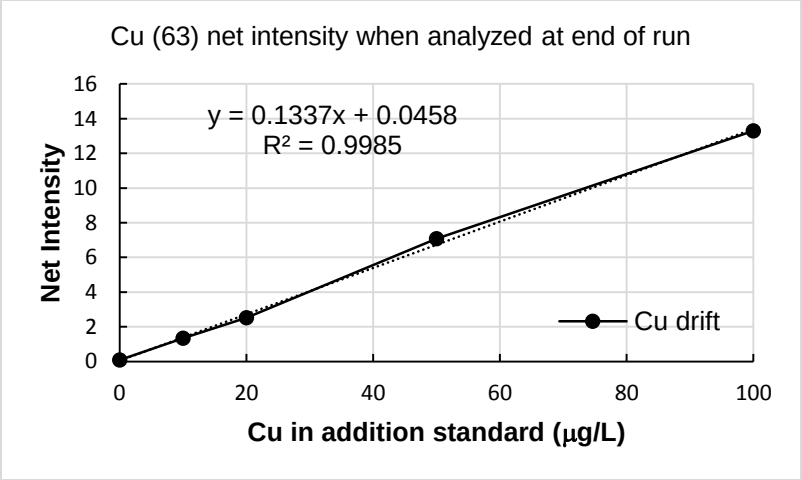

Cu recovery

= 102.4 %

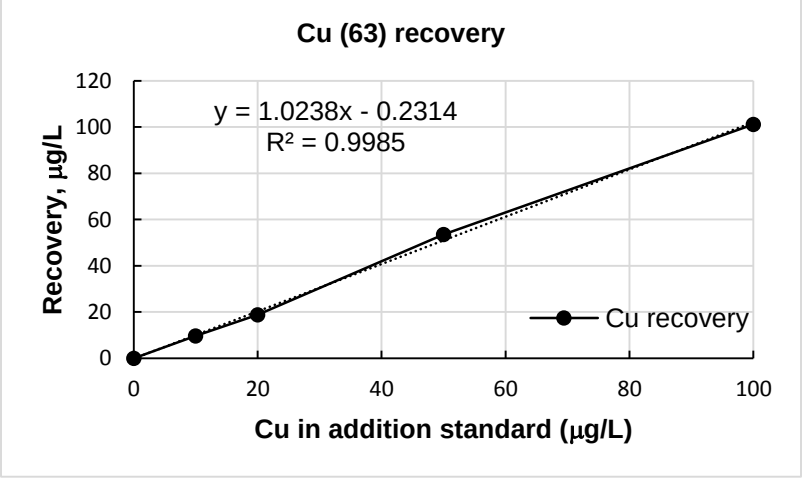

Cu (63) ICP-MS analytical data: calibration curve, drift and recovery estimation

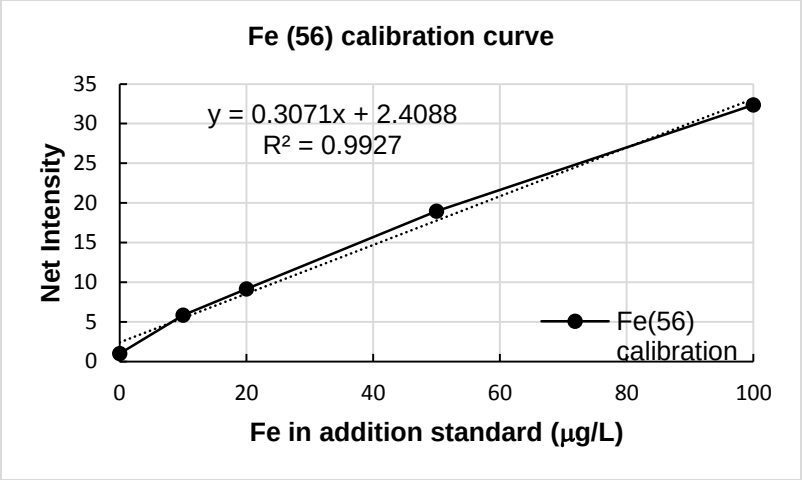

Instrument sensitivity drift for Fe-56

= (0.32 – 0.3071) / 0.3071

= 4.2 %

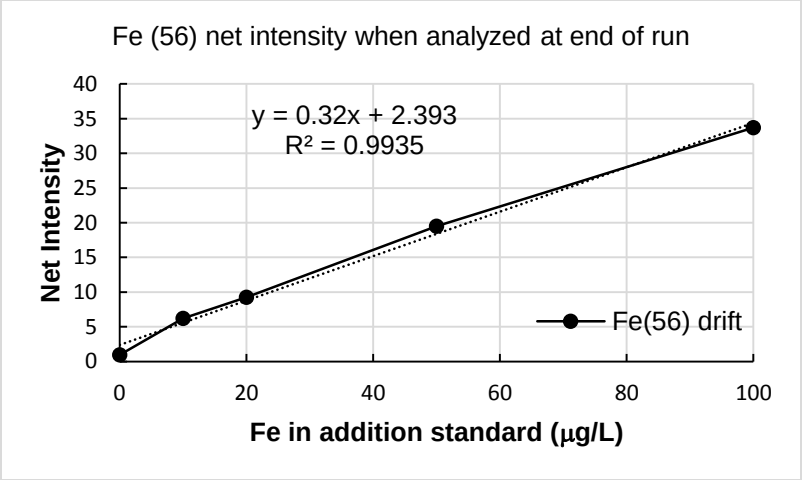

Fe (56) recovery

= 104.2 %

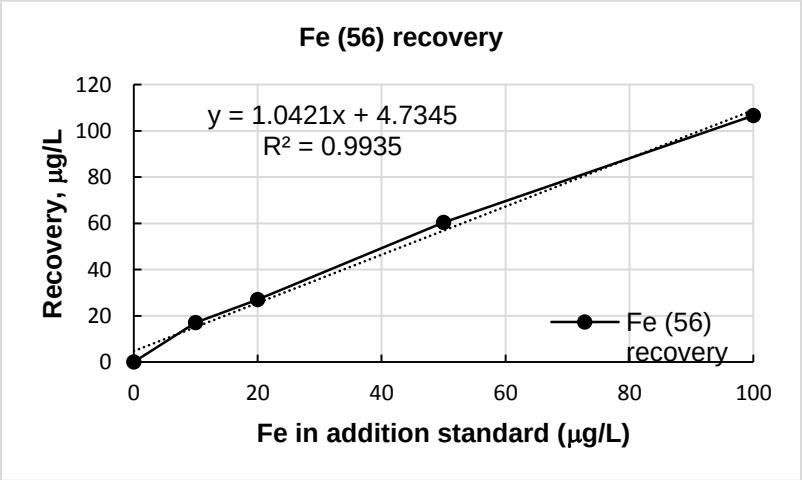

Fe (56) ICP-MS analytical data: calibration curve, drift and recovery estimation

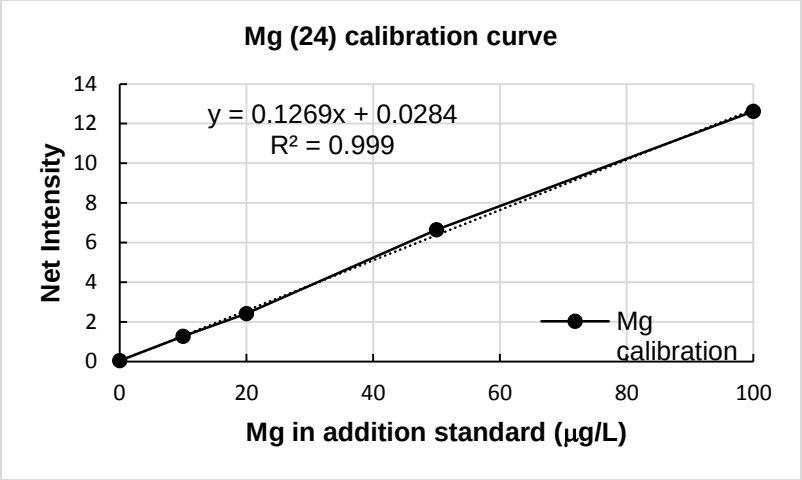

Instrument sensitivity drift for Mg

= (0.1222 – 0.1269) / 0.1269

= -3.7%

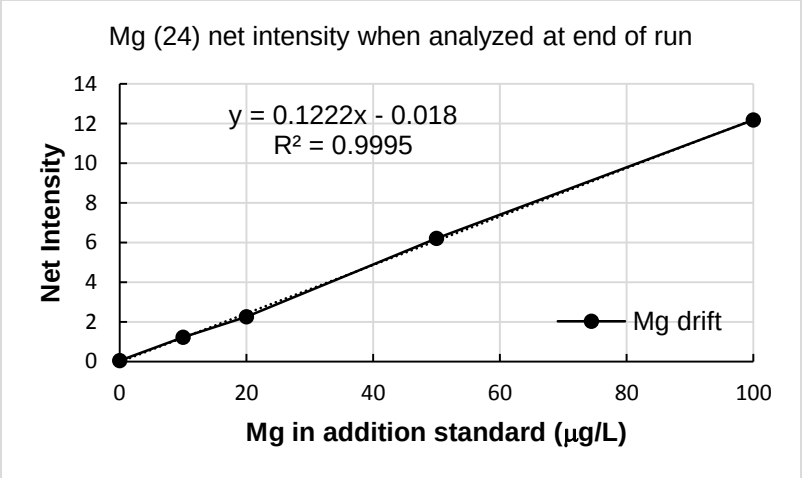

Mg recovery

= 96.3%

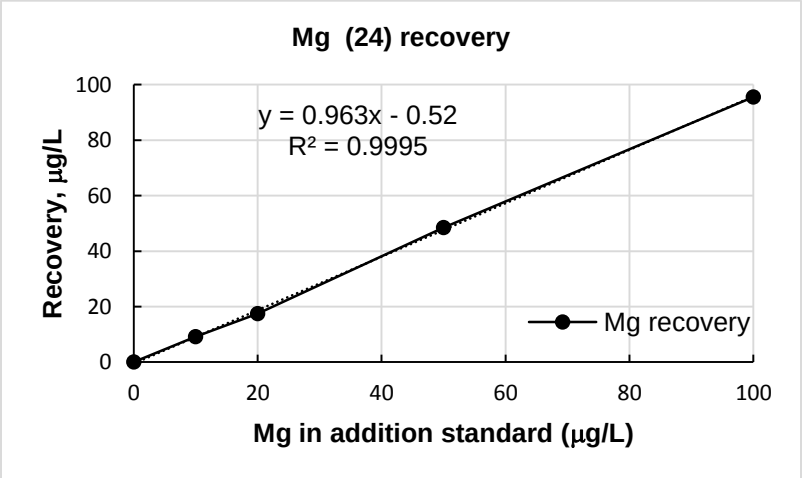

Mg (24) ICP-MS analytical data: calibration curve, drift and recovery estimation

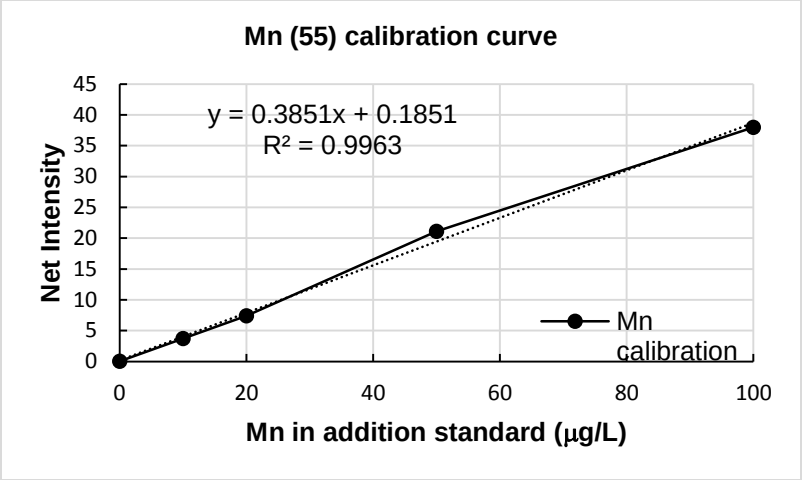

Instrument sensitivity drift for Mn

= (0.3903 – 0.3851) / 0.3851

= 1.35 %

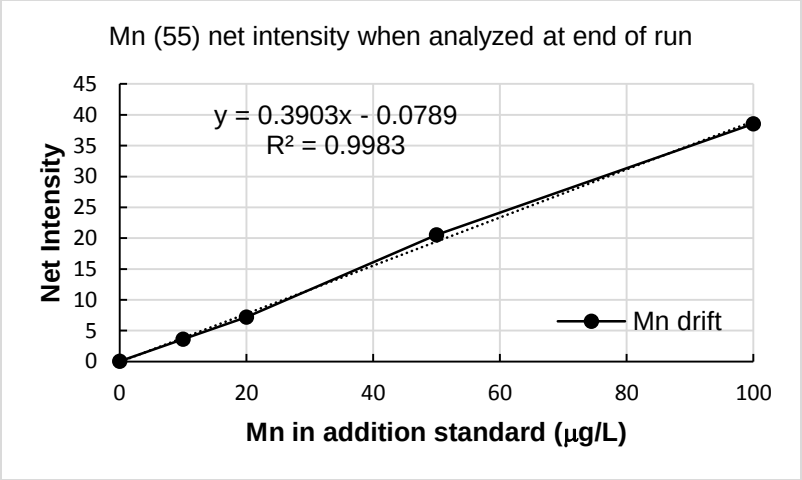

Mn recovery

= 101.3%

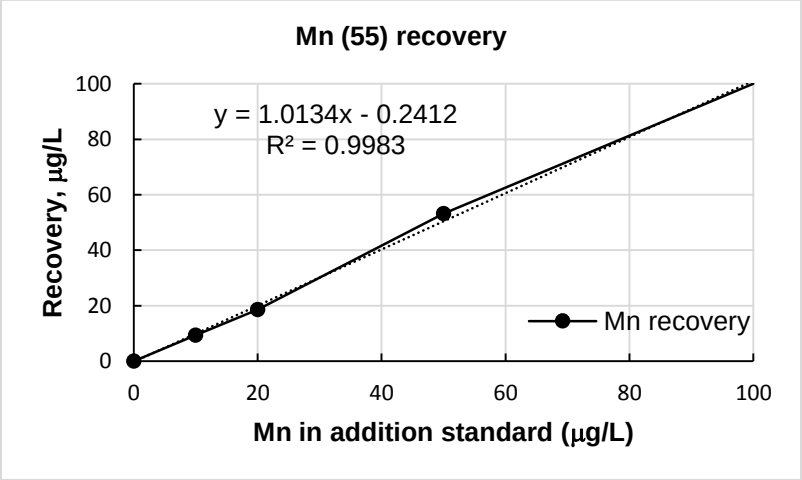

Mn (55) ICP-MS analytical data: calibration curve, drift and recovery estimation

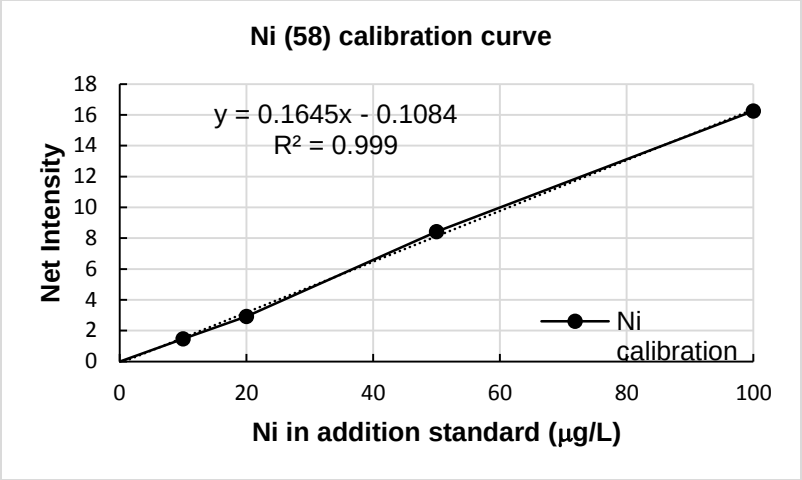

Instrument sensitivity drift for Ni

= (0.1688 – 0.1645) / 0.1645

= 2.61 %

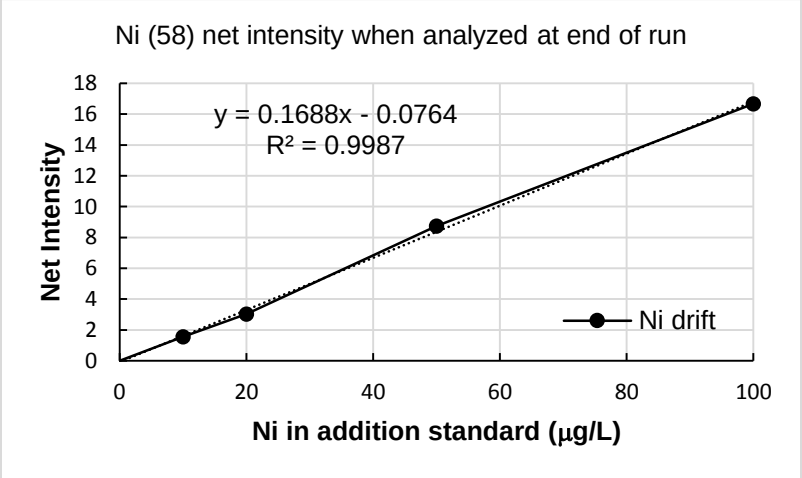

Ni recovery

= 102.6%

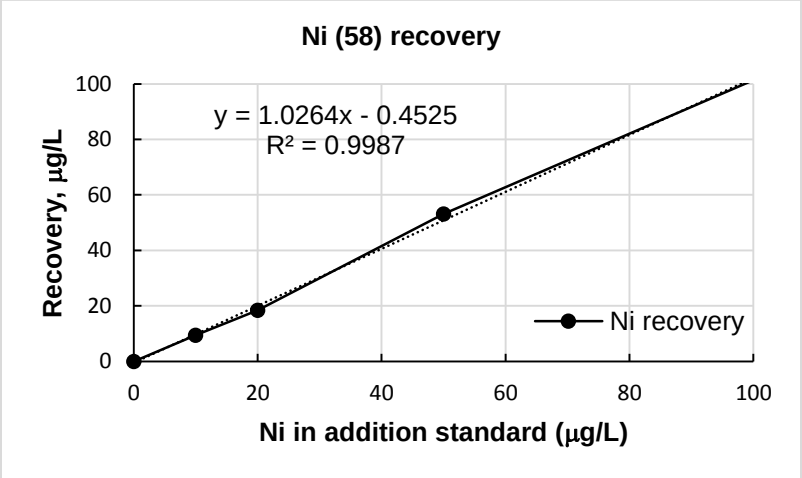

Ni (58) ICP-MS analytical data: calibration curve, drift and recovery estimation

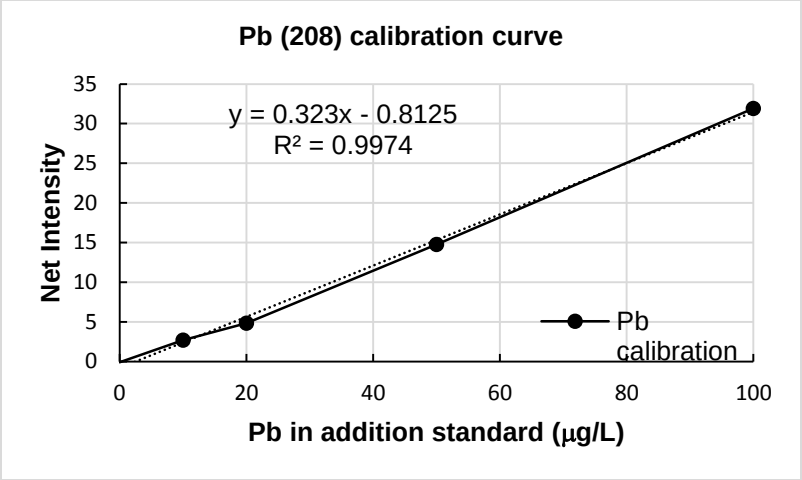

Instrument sensitivity drift for Pb

= (0.3924 – 0.323) / 0.323

= 21.49 %

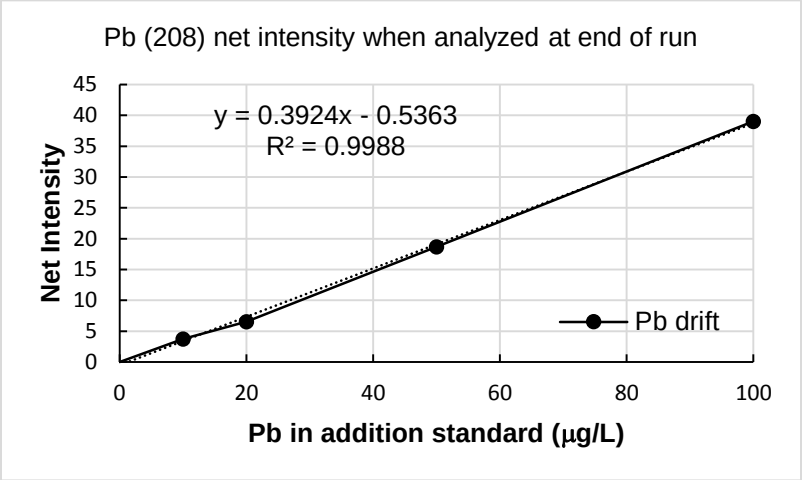

Pb recovery

= 121.5%

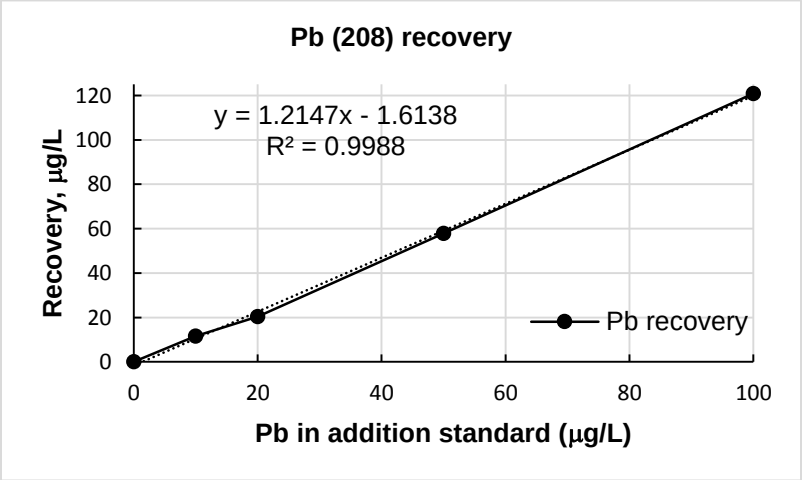

Pb (208) ICP-MS analytical data: calibration curve, drift and recovery estimation

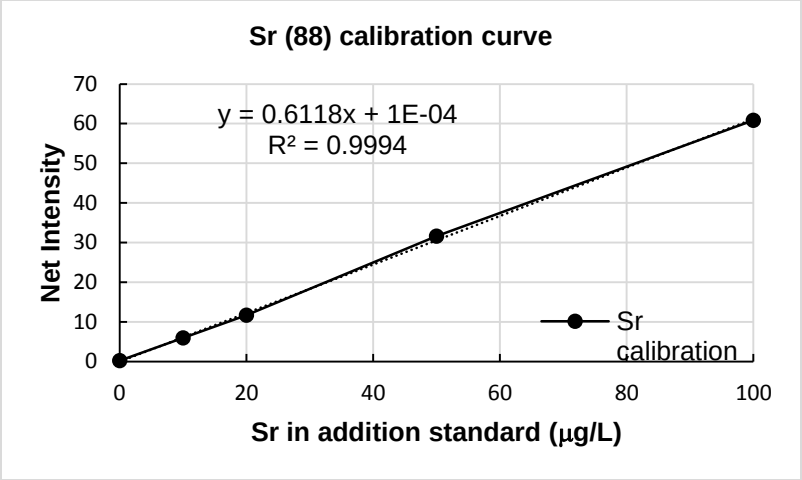

Instrument sensitivity drift for Sr

= (0.632 – 0.6118) / 0.6118

= 3.3%

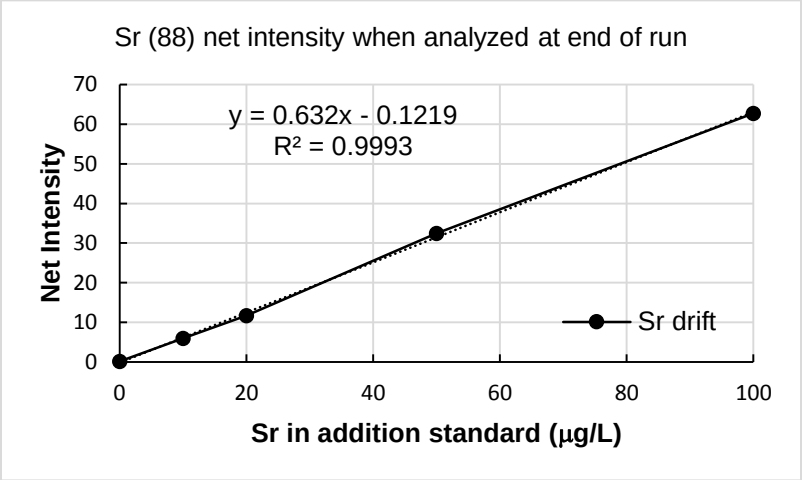

Sr recovery

= 103.3%

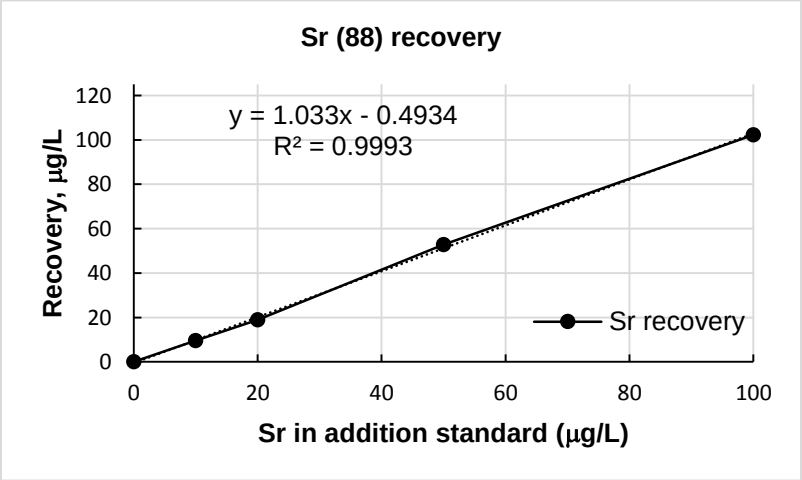

Sr (88) ICP-MS analytical data: calibration curve, drift and recovery estimation

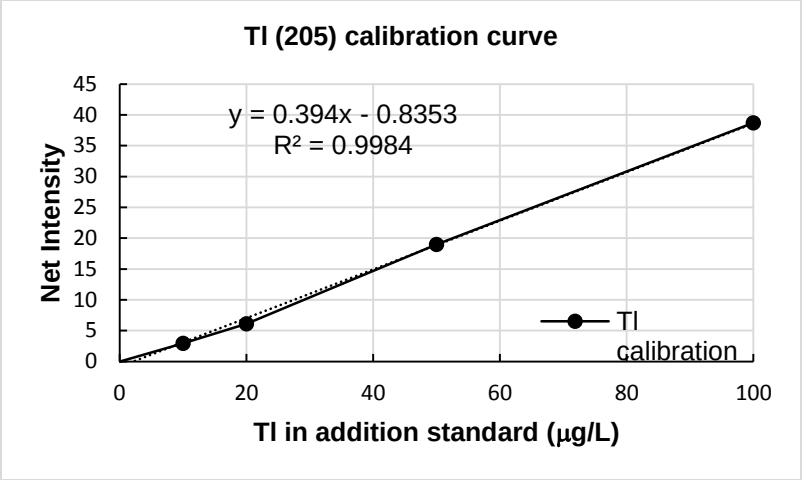

Instrument sensitivity drift for Tl

= (0.4807 – 0.394) / 0.394

= 22.01%

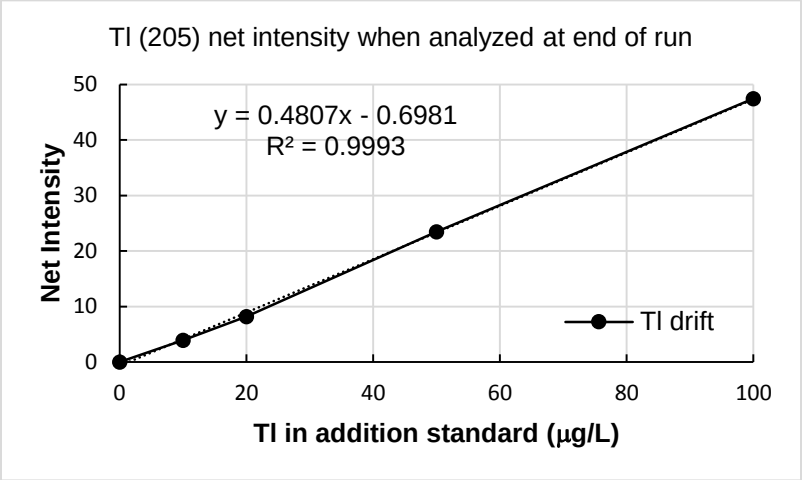

Tl recovery

= 122%

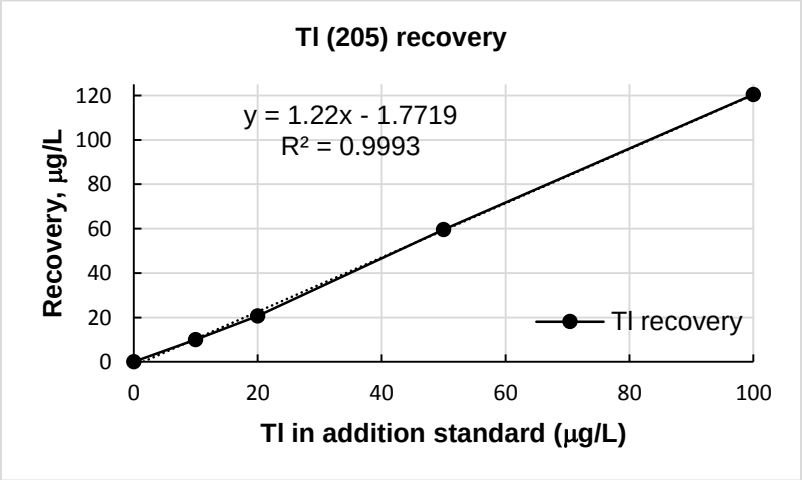

Tl (205) ICP-MS analytical data: calibration curve, drift and recovery estimation

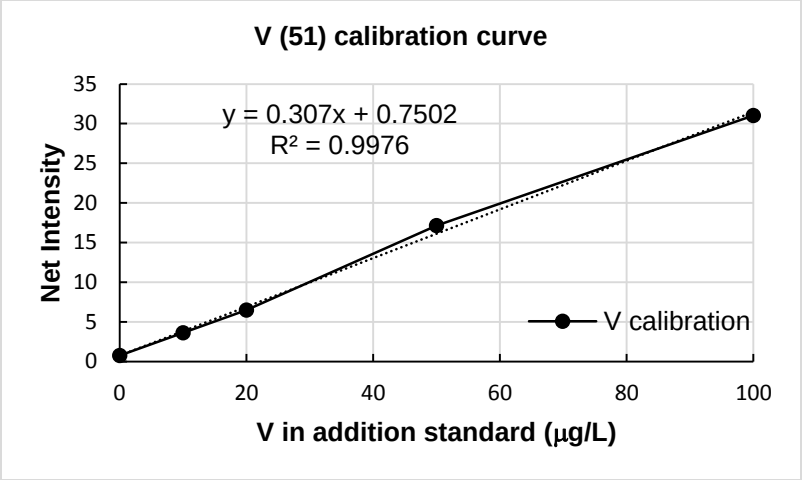

Instrument sensitivity drift for V

= (0.3192 – 0.307) / 0.307

= 3.97 %

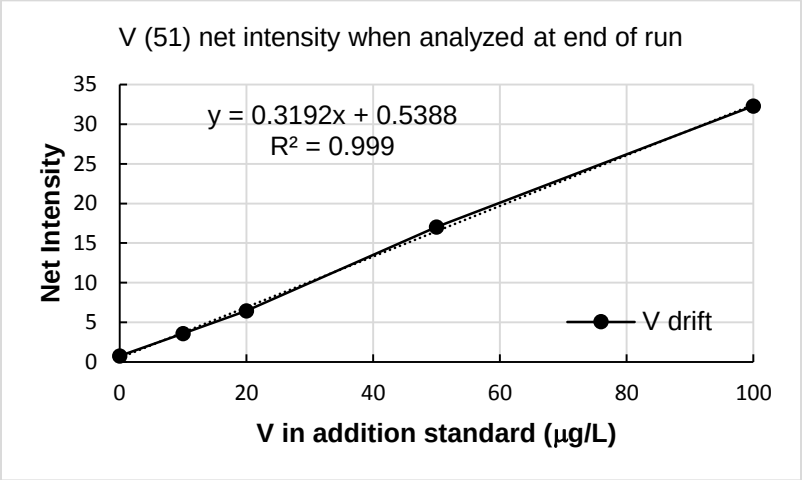

V recovery

= 104 %

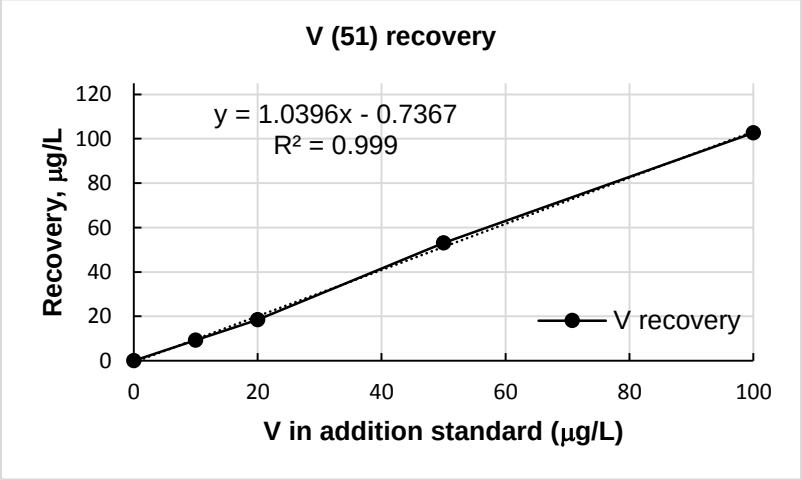

V (51) ICP-MS analytical data: calibration curve, drift and recovery estimation

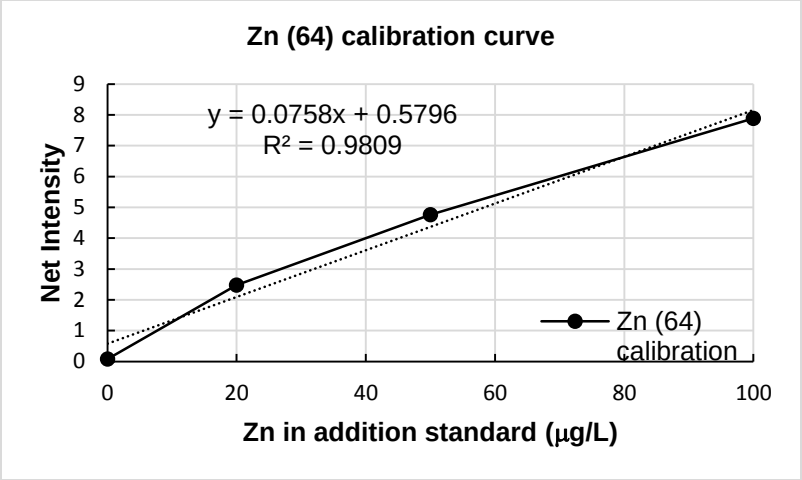

Instrument sensitivity drift for Zn-64

= (0.0762 – 0.0758) / 0.0758

= 0.53 %

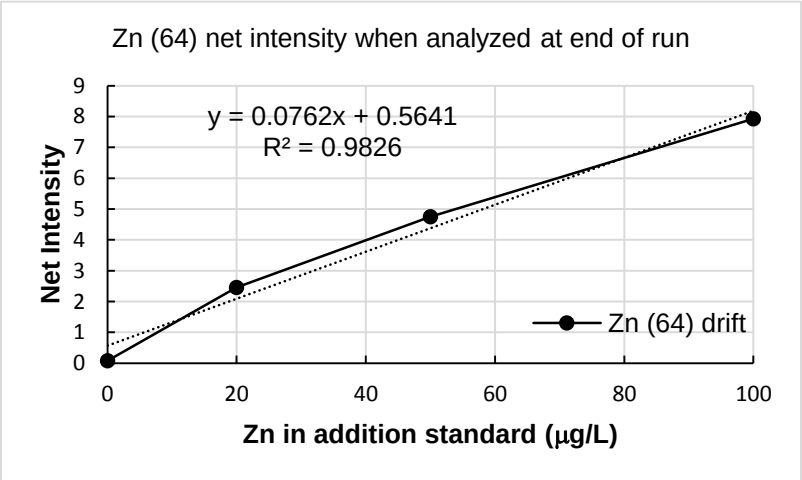

Zn (64) recovery

= 100.5%

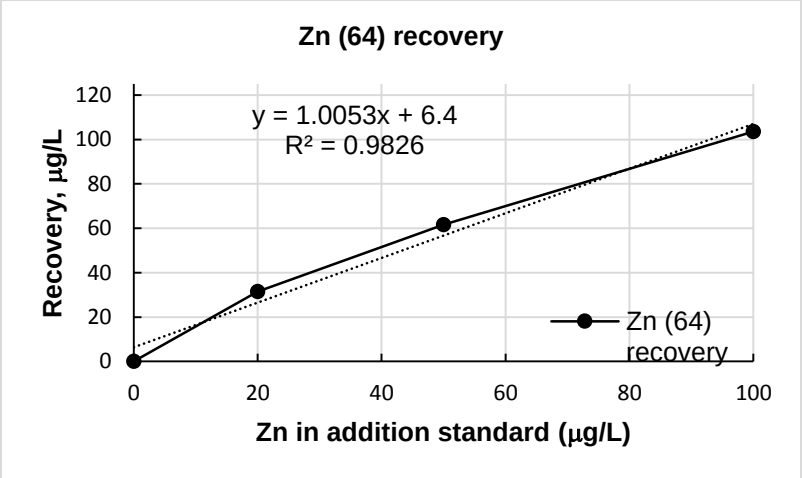

Zn (64) ICP-MS analytical data: calibration curve, drift and recovery estimation

Appendix 2 Explanation to calculate percent groundwater in system

acid addition, ml		Sample withdrawn, ml	System volume, ml	% Groundwater
Incremental	total			
0	0		100	100
2	2		102	98 (=100/102)
		1	101	98
4	6		105	94.3 (=98%*101/105)

Appendix 3 Measured pH, dissolved Si, total Si and percent Si precipitated at each incremental acid addition

Total acid addition, ml A	pH of the mix	Dissolved Si, ppm B	% GW in system C	Total Si concentration in system, mg/l D = Raw GW dissolved Si * C	% Si precipitated E = (D – B)/D
Raw GW*	11.786	25355	100.0	25355	0
2	11.625	25525	98.0	24858	-2.7
6	11.326	26050	94.3	23911	-8.9
8	11.185	24430	92.5	23460	-4.1
10	11.037	23013	90.8	23021	0
11	10.971	18539	89.9	22806	18.7
12	10.933	15849	89.1	22593	29.8
13	10.886	13312	88.3	22382	40.5
14	10.837	10877	87.4	22173	50.9
16	10.760	7033	85.8	21762	67.7
18	10.657	3733	84.3	21363	82.5
21	10.486	810	82.0	20785	96.1
24	9.809	195	79.8	20234	99.0

* Groundwater

Appendix 4 Dissolved Si and percent Si precipitated at each incremental $CaCl_2$ addition

Total $CaCl_2$ addition, g A	Measured pH	Dissolved Si, ppm B	% GW in system C	Total Si concentration in system, mg/l D=Raw GW dissolved Si* C	% Si precipitated E = (D - B) / D
Raw GW*	11.6	40108	100	40108	0%
0.2		38528	100	40108	3.9%
0.4		34949	100	40108	12.9%
0.6		30374	100	40108	24.3%
0.8		27701	100	40108	30.9%
1.0		25494	100	40108	36.4%
1.2		21656	100	40108	46.0%
1.4		17327	100	40108	56.8%
1.6		14336	100	40108	64.3%
1.8		11686	100	40108	70.9%
2.0	11.09	9014	100	40108	77.5%

*GW= groundwater